Responses to the Reviewers

We would like to thank all three reviewers for their thorough comments on this manuscript, which helped to improve the paper. Our responses to general and specific comments are below.

The comments of the reviewers are printed in bold. All line numbers in bold refer to the original manuscript, all others to the revised version.

Reviewer 1

Reviewer general comments: This is a very solid study with important new results on the aerosol in the summer Arctic and its possible sources and effects. Besides the few detailed comments listed below I only have one major issue. Why were the rich and unique data on aerosol composition only discussed in connection with the case study and not also in the discussions of air masses? Recommendation: Accept with modifications and complementing discussion of aerosol composition.

Response - We want to thank Dr. Heintzenberg for his comments on this manuscript. With respect to his major point, we agree that there is also a complementary data set from the AMS that flew on the POLAR6 during the summer campaign. As he points out, we include those data only in the discussion of the case study over the western end of Lancaster Sound. The major reason to not include the AMS dataset for the entire campaign is that the paper was largely focused on the ultrafine particles for which the AMS does not provide direct composition measurements (with the aerodynamic inlet measuring aerosol composition with unity transmission efficiency from just above 100 nm to 700 nm). As well, the AMS data set is extremely full and is being analyzed for presentation as either one or two separate, stand-alone papers. This future work will address the sulfate, organic, ammonium, and MSA aerosol mass concentrations in the campaign. As well, detailed sourcing via investigating the relationship of the aerosol composition to the time spent previously in marine boundary layers (or over other terrain) will be accomplished with FLEXPART-WRF analyses. This new analysis is well beyond what could have been included in the present paper, which is already quite long. We included just a small subset of the AMS data in the present paper to complete the discussion of the case study.

Each of the additional points is addressed below:

Line 46 - Please cite the references that established the phenomenon of Arctic haze long before your first citation.
Response – There are many such references, and we selected the following four for inclusion here on lines 49-50 of the revised manuscript:

- Rahn, K. A., Borys, R. D. and Shaw, G. E.: The Asian source of Arctic haze bands, Nature, 268, 713-715, doi: 10.1038/268713a0, 1977.
- Heintzenberg, B. J.: Particle size distribution and optical properties, Tellus, 32, 251–260, 10.1111/j.2153-3490.1980.tb00952.x, 1980.
- Shaw, G.E. and Stamnes, K.: Arctic haze: perturbations of the polar radiation budget. Ann. N. E Ad. Aci. 338, 533-539, doi: 10.1111/j.1749-6632.1980.tb17145.x 1980.

- Barrie, L. A.: Arctic air pollution: An overview of current knowledge, Atmos. Environ., 20(4), 643–663, doi:10.1016/0004-6981(86)90180-0, 1986.

Line 52 - Again, the influence of the Arctic front has been published about decades before your first citation.
Response – Here, reference to Barrie (1986) has been included on line 53.

Line 85 - Define "main mode number density".
Response – We have removed bracketed terms. The terms "accumulation" and "Aitken" are sufficient here.

Line 91 - There is another, more general, explanation, (see Heintzenberg and Leck, 1994)
Response – Reference added at line 96 with text as follows: "and marine biogenic sulphur (Heintzenberg and Leck, 1994). "

Line 116 - To be complete you might want to cite Heintzenberg et al. (1991) even though no size distributions were measured.
Response – Reference and the following text added on lines 122-126: "Although no size distribution measurements were performed, Heintzenberg et al. (1991) measured vertical profiles of the total particle number concentration greater than 10 nm during June and July, 1984 over the Fram Strait-Spitsbergen area, and found a "rather uniform distribution" with altitude. Their measurements, however, were confined to 500 m-MSL and above."

Line 151 - Where do these transmission data come from?
Response – Reference to Leaitch et al. (2016) added on line 162.

Line 152 - There must have been a substantial temperature increase from ambient to inside the CPC. Did you estimate the potential shrinking and loss of volatile particles due to this temperature increase?
Response – We have not, but we have added a brief discussion of this point beginning on line 162: "Although the transfer of the aerosol from outside to the instruments is relatively fast (5 seconds and less), volatilization of some components of the particles may have occurred. However, it has been demonstrated that the growth of smaller particles by organic condensation occurs primarily by low volatility organic components (e.g. Pierce et al., 2012). Thus, the integrity of the smaller particles that are the focus of the discussion here is more likely to have been maintained. We do expect increasing line losses of particles with sizes decreasing from 10 nm. Therefore our observations will underestimate $N_{5\text{-}20}$."

Line 182 - "Floe"?
Response – Corrected to "flow" on line 198.

Line 384 - Explain "SIL" in text and figure
Response – SIL removed, and replaced with defined BL (boundary layer).

Line 545 - No "loadings", please!
Response – Changed 'loadings' to "mass concentrations" on lines 577-578.

Line 792 - No citations “in prep.”, please!
Response – Removed from reference list and changed to personal communication on line 590-591 and on line 710.

Responses to the Reviewers

We would like to thank all three reviewers for their thorough comments on this manuscript, which helped to improve the paper. Our responses to general and specific comments are below.

The comments of the reviewers are printed in bold. All line numbers in bold refer to the original manuscript, all others to the revised version.

Reviewer 2

Reviewer general comments: This paper investigates ultrafine particle (UFP) concentrations in the Canadian Arctic through aircraft measurements. The topic is of interest and important given the rapid changes expected for this region. Overall, I think an attempt at a more quantitative analysis, a more in-depth discussion of the limitations of the approach used in this work, (given that this has been grappled with and addressed in the past literature) and a more complete citation of the existing publications on this topic is needed.

A stated goal is to understand new particle formation (NPF) events (ie, the source of UFP) and how they evolve (grow) to affect radiative forcing through acting as CCN.

The paper really mainly focuses on the NPF events. A number or instruments were deployed, most important for addressing this question are measurements of all particle number concentrations larger than 5nm and number size distributions of particles larger than 20 nm. By difference, the authors determine the number between 5 and 20 nm to assess NPF. There is a substantial body of published literature on the the subject of investigating NFP using difference measurements, ie, typically this was done by subtracting data from a UFCPC (eg, TSI 3025) and CPC (eg, TSI 3010 or similar), to obtain concentrations of particle in the 3 to 10 nm range, and the limitations with this type of difference approach. In this study, these limitations are more severe as UFPs are defined over a larger size range, 5 to 20 nm, and smallest size is higher, 5 nm, further away from the size of the newly nucleated particle (1 to 1.5 nm). Furthermore, there are no measurements of possible nucleation gas-phase precursors, such as sulfuric acid, (or SO2 and estimated OH could work, but not as well), ammonia and possible low volatile VOCs. Since new stable particles have sizes near 1 or so nm, and in pristine environments particle growth rates can be slow, it can take considerable time for the NPF event to be observable with the the deployed instrumentation. This make interpretation of this data very challenging for investigating nucleation conditions. Thus, essentially, the authors instrumentation is not ideal for addressing the scientific aim of defining NPF conditions in the Arctic.

First, it is recommended that the authors present a thorough assessment of the limitations with their method. This should include: 1) An analysis of the LOD of the difference method used to determine N(5-20) is needed. This will likely show that only significant concentrations of N(5-20) particles can be detected with certainty, potentially leading to a view biased by focusing only on larger nucleation events, which should be discussed. (This should likely include uncertainty in counting statistics, integrated size distributions to get total N of the measured distribution, N20, both instrument flow uncertainties, errors associated with subtracting two large numbers of small difference, etc. 2) The uncertainty in conditions that actually existed at time of the NPF event versus what

existed at the time of the measurement due to expected times between the two (ie, if possible, estimate the delay from nucleation to detection based on estimated or assumed growth rates of nanoparticles).

Without measurements of possible new particle precursor gases and lack of particle concentrations near the critical nucleation diameter it is very difficult to discuss conditions leading to NPF with certainty. For example, it is noted that often an inverse relation is seen between N(5-20) and larger particle concentrations. This could be due to formation of these smaller particles in cleaner air (ie, nucleation precursor vapors can build up due to lack of vapor condensational sink), or the new particles in the cleaner region just have a longer life span compared to particles that may have been formed in the other regions that had higher concentrations of pre-existing particles, which depleted the N(5-20) particles faster. Thus, how can one conclude that the only particle formation events are in the clean regions (possible confirmation bias). I think the authors have provided evidence that UF particles are generated in the Arctic BL and it can occur under clean conditions, but what happens in more polluted air masses is not really known. Specifically, how (by what process), under what conditions (where), is not definitively known. More analysis, involving calculations (estimations) of lifetimes, more discussion of possible differences in measured total particle surface areas between regions, may allow more definitive conclusions. Some data is clearly not available to make more quantitative assessments, but maybe typical values reported in clean similar environments can set a bound.

Finally, it is not clear what is special about the clouds that leads to NPF in their vicinity. Since this is one major finding of this paper, more details are warranted, including a more comprehensive analysis of the literature, eg; [Clarke et al., 1999a; Clarke et al., 1999b; Hegg, 1991; Hegg et al., 1990; Hoppel et al., 1994; Mauldin et al., 1997; Perry and Hobbs, 1994; Radke and Hobbs, 1991; Raes, 1995; Weber et al., 2001; Wiedensohler et al., 1997]

Responses – We thank the reviewer for their comments, which help to improve the paper. The following are a few responses to the reviewer's more general comments:

1) As discussed below, we have included some of the additional references the reviewer suggests.

2) We agree with the reviewer that growth rates may be slower in pristine environments. However, in this study we were apparently very close to a source of particle precursors (biologically productive sea and sea-ice interface). In other words, we were not necessarily pristine from the point of view of potential precursors, even though we were pristine by comparison with anthropogenic environments. The work of Willis et al. (2016) illustrates rapid aerosol growth in this environment.

The main point of the paper is to demonstrate that ultrafine particles are associated with the ocean surface during the Arctic summer when particle mass concentrations are extremely low. Airborne measurements of NPF associated with open water in the Arctic are surprisingly few: Leaitch et al. (1983 and 1994). This work offers a unique perspective on the issue. With respect to growth of the particles to reach 5 nm and beyond 20 nm, we note that in the absence of significant coagulation (the effect of which will be reduced due to the relatively low

concentrations of particles smaller than 20 nm) it requires more than 100 times more condensable precursor for particles to grow from 20 nm to 50 nm compared with particles growing from 1 nm to 10nm. Willis et al. (2016) showed that for this environment particles were able to grow to 50 nm low over the open water over approximately one hour, which means that the growth from 1 nm to 10 nm can occur over one minute or less, justifying our use of instruments that are sensitive to 5 nm particles and larger. Of course, we would have very much have liked to have instruments operating sensitive to 1 nm particles but they were not available to us for this study. It is our belief that doing the first systematic altitude-resolved study of particle size distributions in the summertime Arctic marine environment with a standard set of instrumentation makes this work noteworthy.

Also, please note that we may have misled readers (and the reviewer) of the ACPD version of the paper by averaging all data in our vertical profiles, which led to a bias by overweighting single flights at some altitude intervals. We apologize for this. The new averaging method used in the revised manuscript equally weights data from all flights at all altitudes intervals. We added a brief description to the paper (line 244-249): "An average profile for a single flight was obtained by binning all data from the respective flight into altitude intervals of 100m starting at the lowest flight altitude. In addition to data obtained during vertical profile flights, data acquired while flying at a constant level were also included. Average profiles containing data of more than one flight were calculated by averaging the respective single flight profiles. " We revised all figures showing average profiles (Figure 5-8).

Figure 5 and Figure 8 originally showed that the maximum in the UFP concentration over open water was above the lowest sampling level. To the new version of Figure 8, we have added N_{tot}, which was sampled every second and shows the increase in particles over open water is also associated with the lowest sampling level. That observation is consistent with the results of Willis et al. (2016) as well as past observations related to polynyas (Leaitch et al. 1983 and 1994).

As for the limit of detection, Leaitch et al. (2013) found an average CPC-SMPS of 47/cc for points during dark periods at Alert, Nunavut (1861 one hour averages) with a standard deviation of 73/cc and a 95^{th} percentile of 144/cc, indicating that values of CPC-SMPS in excess of 200/cc are reasonable indicators for NPF. Our discussion on lines 338-345 of the original manuscript (363-370 of revised paper) already addresses this concern.

3) With respect to the reviewer's comments concerning the conditions under which we observe NPF, we now indicate in the Abstract that high levels of UFPs are observed when the condensation sink is smallest, i.e. lowest numbers of larger particles. We feel that this is an accurate short summary, based on the observations made in the study. The reviewer suggests that the "precursor vapors can build up due to the lack of a condensation sink" but it is not clear what sort of 'build up' is needed. The formation of 1000 particles/cc, each of which is 10 nm in diameter, requires very little precursor. Over a biologically productive sea, it is very likely that sufficient precursor will be available for NPF if the condensation sink is low enough, as in the early part of this study.

The reviewer suggests that "the new particles in the cleaner region just have a longer life span compared to particles that may have been formed in the other regions that had higher concentrations of pre-existing particles, which depleted the N(5-20) particles faster." If that were the case, then we would have seen the NPF occur at other locations and not principally associated with the ocean surface.

Finally, the reviewer argues that "what happens in more polluted air masses is not really known". This may be true but we find less evidence for NPF associated with less pristine conditions. It is clear that in this relatively clean background environment, a low condensation sink is a necessary condition. The paper does not address more polluted conditions.

4) As in our response to the reviewer's comment concerning lines 573-575, we have added a sentence to elaborate on the potential role of clouds in this instance (lines 608-611 of the revised manuscript). We use two of the references suggested by the reviewer (one reference the reviewer suggested was already present): Clarke et al. (1999) and Mauldin et al. (1997). These are on lines 601-602 of the revised manuscript. Of course it is not unique that NPF is associated with clouds. We also added two more references suggested by the reviewer that illustrate a connection of new particles with clouds (Radke and Hobbs 1991, Wiedensohler et al. 1997). What is important here is that relative to the cloud-free observations over ice and water, the UFP over cloud were common and the associated concentrations are higher (Figure 8).

References added:

- Clarke, A. D., Kapustin, V. N., Eisele, F. L., Weber, R. J. , and McMurry, P. H.: Particle production near marine clouds: sulfuric acid and predictions from classical binary nucleation, Geophys. Res. Lett., 26, 2425-2428, doi: 10.1029/1999GL900438, 1999.
- Mauldin, R. L., Madronich, S., Flocke, S. J. , Eisele, F. L. , Frost, G. J. and Prevot, A. S. H. : New insights on OH: Measurements around and in clouds, Geophys. Res. Lett., 24(No 23), 3033-3036, doi:10.1029/97GL02983, 1997.
- Radke, F. L. and Hobbs, P. V.: Humidity and particle fields around some small cumulus clouds, Journal of atmospheric sciences, 48(9), 1190-1193, doi: http://dx.doi.org/10.1175/1520-0469(1991)048<1190:HAPFAS>2.0.CO;2, 1991.
- Wiedensohler, A. H.-C. Hansson, D. Orsini, M. Wendisch, F. Wagner, K.N. Bower, T.W. Chourlarton, M. Wells, M. Parkin, K. Acker, W. Wieprecht, M.C. Facchini, J.A. Lind, S. Fuzzi, B.G. Arends, M. Kulmalao: Night-time formation and occurrence of new particles associated with orographic clouds, Atmos. Env., 31(16), 2445-2559, doi: http://dx.doi.org/10.1016/S1352-2310(96)00299-3, 1997.

Specifics:

Reviewer - Lines 73 to 76. These statements are unsupported and possibly not accurate. It all depends on the conditions (thus the statement must be qualified) and also depends on what is defined as ultrafine particles.

Response – We feel these statements are supported by the observations, as discussed above.

Reviewer - Should explicitly calculate estimated losses associated with sampling 5 nm particles (ie, this is the worst case scenario).

Response – In response to Reviewer 1 and this comment, we have added on lines 159-165 of the revised paper: "Although the transfer of the aerosol from outside to the instruments is relatively fast (5 seconds and less), volatilization of some components of the particles may have occurred. However, it has been demonstrated that the growth of smaller particles by organic condensation occurs primarily by low volatility organic components (e.g. Riipinen et al., 2011; Pierce et al., 2012). Thus, the integrity of the smaller particles that are the focus of the discussion here is more likely to have been maintained. We do expect increasing line losses of particles with sizes decreasing from 10 nm. Therefore our observations will underestimate $N_{5\text{-}20}$."

Reviewer - For given AMS LODs, what was the AMS sampling rate.

Response – The sampling rate was 30 seconds. This has now been added to the paper (line 222).

Reviewer - Was N(tot) every defined? Ie, what is the smallest size.

Response – Yes, it was defined on line 179 of the ACPD manuscript as the UCPC measurement, which on line 176 refers to particles larger than 5 nm. In addition, we have added on lines 194-196: ", noting as above that diffusional losses of particles smaller than 10 nm make the Ntot observations lower limits."

Reviewer - Line 339, what exactly does a burst of N(5-20) mean, was it a burst because the aircraft flow through a small region of high concentrations, or is it being implied that there was a burst in NPF? If the latter, how is that known? In fact, the use of "burst" throughout the paper is confusing since what it really means is isolated regions of high UF particles were encountered, not the typical meaning of a large nucleation event occurring over a short period of time (which I believe is what is implied). It is not clear that the latter can be determined from this sampling approach.

Response – Bursts here refers to sudden increases in N5-20. We have clarified that on line 359-361 of the revised manuscript by the addition of "Here we refer to "bursts" of particles as a sudden and relatively large increase in $N_{5\text{-}20}$. This may reflect inhomogeneities in the NPF process or may reflect the aircraft flying in and out of a NPF event."

Reviewer - Lines 350: on possible reasons for high fractions of UF particles; this could also include, very slow growth rates, biased aircraft sampling (ie, you went looking for them).

Response – As above, the results in Willis et al. (ACP, 2016) do not suggest very slow growth rates, and we do not include that as a possibility. We agree that there could be some bias associated with our sampling, and accordingly we have added the following sentence to lines 379-381 of the revised manuscript: "Also, since observations of UFP were one focus of this study, the fractional occurrence of the UFP mode may be slightly biased due to longer sampling times associated with UFP occurrence."

Reviewer - Lines 462-465. This sentence seems to exactly confirm the limitations with the analysis used in the paper; the presence of UFP may have mostly to do with residence time in the BL and not mechanism that formed them.

Response – If these particles were resident for a long time in the BL, then we should have observed them everywhere. But this was not consistent with the observations.

Reviewer - Line 497-498; This conclusion is not the only possible one, it is also possible that they just are not scavenged and so have a longer life time (as noted already). Without measuring the nucleation precursor species, it is hard to tell. Calculations of life times of particles of 5 to 20nm due to coagulation, based on given size distributions may be insightful. Growth out of the 5 to 20 nm size range due to condensation is likely more important. Maybe if some assumptions are made on typical concentrations of H2SO4 or low volatile VOCS one could also estimate this, or use reported growth rates in other clean regions?

Response – Our response is the same as to the comment immediately above as well as our above responses to the reviewer's general comments.

Reviewer - Lines 573-575 and 594-595. Not clear what the all the ideal conditions for NPF were, is it just high OA levels? More details would be good, see references (eg, precipitating clouds scavenge accumulation mode aerosols, reducing surface area, but nucleation precursor gases can pass through (eg, SO2) forming H2SO4 in the high OH (high actinic flux and RH) in the cloud outflow, plus high RH leads to NPF…

Response – Thank you. We have added the following on lines 608-611 of the revised manuscript: " In other words, precipitating clouds scavenge aerosol particles, reducing the surface area for condensation, but some fraction of nucleation precursor gases with lower Henry's Law constants can pass through (e.g. SO_2) leaving the potential for H_2SO_4 in the higher OH in the cloud outflow (a discussion of the processes can be found in Seinfeld and Pandis, 1998)."

Reviewer - Lines 647-648: I think this sentence should be clarified. It cannot be said that the open water is the source of the observed particles, it may be true, but it could also be that stable new particles of sub 5 nm size were formed elsewhere and just grew to your detectable size due to ocean emissions.

Response – See response to above comment concerning lines 462-465 and our above responses to your general comments.

References

Leaitch, W.R., Hoff, R.M., Melnichuk, S., and Hogan, W.: Some chemical and physical properties of the Arctic winter aerosol in northeastern Canada. J. Climate Appl. Meteorol., 23, 916-928, http://dx.doi.org/10.1175/1520-0450(1984)023<0916:SPACPO>2.0.CO;2, 1984.

Leaitch, W.R., Barrie, L.A., Bottenheim, J.W., Li, S.-M., Shepson, P. and Yokouchi, Y.: Airborne observations related ozone depletion at polar sunrise. J. Geophys. Res., 99, 25499-25517, 10.1029/94JD02750, 1994.

Leaitch, W. R., Sharma, S., Huang, L., Toom-Sauntry, D., Chivulescu, A., Macdonald, A. M., von Salzen, K., Pierce, J. R., Bertram, A. K., Schroder, J. C., Shantz, N. C., Chang, R. Y. W. and Norman, A.-L.: Dimethyl sulfide control of the clean summertime Arctic aerosol and cloud, Elem. Sci. Anth., 1(1), 17, doi:10.12952/journal.elementa.000017, 2013.

Willis, M. D., Burkart, J., Thomas, J. L., Köllner, F., Schneider, J., Bozem, H., Hoor, P. M., Aliabadi, A. A., Schulz, H., Herber, A. B., Leaitch, W. R. and Abbatt, J. P. D.: Growth of nucleation mode particles in the summertime Arctic: a case study, Atmos. Chem. Phys., 7663–7679, doi:10.5194/acp-16-7663-2016, 2016.

Responses to the Reviewers

We would like to thank all three reviewers for their thorough comments on this manuscript, which helped to improve the paper. Our responses to general and specific comments are below.

The comments of the reviewers are printed in bold. All line numbers in bold refer to the original manuscript, all others to the revised version.

Reviewer 3

We thank the reviewer for their comments.

Reviewer: As a description of a flight campaign this manuscript includes a lot of information and the authors should have credit for trying to limit what is probably much more than enough behind the scene. Just as using cloud probes as a tool to stratify cloudy or non-cloudy measurement I see no problem of using differences between instruments as indicators for NPF (despite any measurement problems). The absolute numbers are really not followed up in the work. Hence, I will not dwell on measurement details.

Response: We thank the reviewer for their perspectives on the measurement approaches used in the study. We also believe also that there is merit to using the difference between the numbers of particles between 5 and 20 nm, i.e. $N_{5\text{-}20}$, to study the nature of aerosol processes as a function of location and height in this high Arctic regime. In our response to Reviewer 2, we discuss further the merits of this approach.

Reviewer: What I am missing is a Reader's Digest for modelers. Much of what is presented was already observed during previous campaigns, but the wealth of data could be presented in a summary nicely arranged with pertinent chemical and thermodynamically properties.

Response: This is a very good point, and so we have re-written the abstract of the paper and tightened the language in the conclusions section. Overall, we believe that the main points ("Readers Digest") of the study that a modeler should take away are that: 1) new particle formation occurs readily in the Canadian high Arctic boundary layer, a region dominated by marine and coastal regions, 2) particle growth also occurs in these regions under specific environments, 3) the highest levels of ultrafine particles were associated with above-cloud conditions influenced by marine air, and 4) ultrafine particle formation occurs much less frequently in the free troposphere under these conditions. Modeling efforts would ideally represent such behavior but are currently limited by our knowledge of marine aerosol precursor emissions.

That all said, we actually disagree that much of what we have observed has been seen before. In particular, this is the first systematic altitude-resolved study of the nature of ultrafine particles in mid-summer in the high Arctic. As we responded to Reviewer 2, what is important here is that relative to the cloud-free observations over ice and water, the UFP over cloud are common and the associated concentrations are higher (Figure 8). Also, in both the cloud and open water cases, the highest UFP concentrations are found at the lowest measurement levels, implying that the

surface (water or cloud) is critical to the NPF process. It is information of this type that is needed for comparisons against model output, to test the validity of the model representations of aerosol processes.

Reviewer: These cases could then be tried and tested using models. The aim in the beginning of the manuscript states a focus on UFP and this is ok, but quantifying their potential impact requires a model. The processes are very complex, and any changes in cloud base height for instance will over compensate any aerosol effect. Again, a model is needed.

Response: While the impacts of the UPFs are certainly interesting and have motivated this study to a large degree, it was beyond the scope of this observational paper to include the impacts that can only be evaluated with a model. However, we make reference to the work of Leaitch et al. (2016) that has pointed out that particles as small as 20 nm become activated into cloud droplets in this environment, motivating potential impacts and the needed to understand the processes that lead to their formation. Also, we now refer to Croft et al. (2016) that models one significant impact of NPF on Arctic radiative forcing.

Reviewer: I'm not convinced the CCN chapter of the manuscript is required for the NPF focus. In my opinion, the papers stands well as a description of the campaign, but I would prefer that the paper takes the understanding further than that of Shaw, Atmospheric Environment Vol. 23, No. 12, pp. 284-2846, 1989. What extra knowledge stands out form these flights besides, low mixing, low surface area, high insolation? A summary of this specifically would be a nice contribution. I don't contest that it is in the manuscript, but it could be summarized in a nice form.

Response: We agree that Shaw nicely illustrated that particle nucleation may occur in clean atmospheric environments, such as those in polar regions that have experienced recent scavenging. So, in that context, we fully agree that there are no new conceptual findings in our work compared to this work by Shaw, and other, earlier studies. However, what is new in this work are actual measurements of ultrafine particles in the high Arctic summer, especially in an altitude-resolved manner. These have not been documented so clearly before and such information is needed to compare against model output. Further, the work contrasts NPF over three different surfaces (ice, water and top of low cloud) in the same environment, which has never been done before and is important. We don't have sufficient statistics to conclude that the low cloud presence enhances the NPF relative to open water, but that certainly is the indication.

While we also agree that the CCN measurements are in some sense disconnected from the focus on the paper on the UFPs, we prefer to leave them in the paper as an illustration of the numbers of particles that may be arising, in part, from the growth of the UFPs that were measured. In order to improve the connection between the UFP observations and the CCN, we have added Figure 12 that shows correlations among the smaller particle sizes and the CCN. We also emphasise that the CCN measured here are larger than the average size of particle found by Leaitch et al. (2016) to participate in cloud droplet nucleation.

Reviewer: Orography is a source for concern at Svalbard, what about the conditions at the flight campaign?

Response: This is an interesting point re. orography. It is true that the nucleation and growth event documented in Willis et al. occurred in air that had resided over Devon Island (maximum altitude 2000 m) before descending through katabatic flow to the Lancaster Sound, and the same is evident in the event documented in Figure 8 of the present paper. Such air may have been cleaned by passing through this higher elevation location, lowering its condensation sink. However, aside from whatever reduced the condensation sink, the surfaces appear to be the sources of the particle precursors.

Reviewer: Ström et al. 2009 fig 11 Tellus would be nice to compare directly with the supplement figure 1. The fact that Aitken mode particles are not observed right at the surface could be an instrument detection issue I guess. Particles must grow to detectable size. On the source of particle near the surface, have a look at: Lampert et al., Inclined Lidar Observations of Boundary Layer Aerosol Particles above the Kongsfjord, Svalbard As an example of ocean source. Acta Geophysica 60(5), October 2012.

Response: This is a very valuable point, that it is possible that particles nucleate at the surface but require time to growth to sizes that are detectable. However, as referred to in our response to Reviewer 2, we apologize because we have now improved our profile averaging approach. We have revised Figure 8, which originally showed that the maximum in the UFP concentration over open water was above the lowest sampling level. That was due in part to a bias associated with the averaging time of the SMS, which has been removed. To Figure 8, we have now added N_{tot}, which was sampled every second and shows the increase in particles over open water is also associated with the lowest sampling level. That observation is consistent with the results of Willis et al. (2016) as well as past observations related to polynyas (Leaitch et al. 1983 and 1994).

References

Leaitch, W.R., Hoff, R.M., Melnichuk, S., and Hogan, W.: Some chemical and physical properties of the Arctic winter aerosol in northeastern Canada. J. Climate Appl. Meteorol., 23, 916-928, http://dx.doi.org/10.1175/1520-0450(1984)023<0916:SPACPO>2.0.CO;2, 1984.

Leaitch, W.R., Barrie, L.A., Bottenheim, J.W., Li, S.-M., Shepson, P. and Yokouchi, Y.: Airborne observations related ozone depletion at polar sunrise. J. Geophys. Res., 99, 25499-25517, 10.1029/94JD02750, 1994.

Willis, M. D., Burkart, J., Thomas, J. L., Köllner, F., Schneider, J., Bozem, H., Hoor, P. M., Aliabadi, A. A., Schulz, H., Herber, A. B., Leaitch, W. R. and Abbatt, J. P. D.: Growth of nucleation mode particles in the summertime Arctic: a case study, Atmos. Chem. Phys., 7663–7679, doi:10.5194/acp-16-7663-2016, 2016.

Marked-up Manuscript

Changes are highlighted in yellow.

Summertime observations of elevated levels of ultrafine particles in the high Arctic marine boundary layer

Julia Burkart[1], Megan D. Willis[1], Heiko Bozem[2], Jennie L. Thomas[3], Kathy Law[3], Peter Hoor[2], Amir A. Aliabadi[4], Franziska Köllner[5], Johannes Schneider[5], Andreas Herber[6], Jonathan P. D. Abbatt[1], W. Richard Leaitch[7].

[1] {Department of Chemistry, University of Toronto, Toronto, Canada}

[2] {Institute of Atmospheric Physics, Johannes Gutenberg-University, Mainz, Germany}

[3] {LATMOS/IPSL, UPMC Univ. Paris 06 Sorbonne Universités, UVSQ, CNRS, Paris, France}

[4] {Environmental Engineering Program, University of Guelph, Guelph, Canada}

[5] {Particle Chemistry Department, Max Planck Institute for Chemistry, Mainz, Germany}

[6] {Alfred Wegener Institute, Helmholtz Center for Polar and Marine Research, Bremerhaven, Germany}

[7] {Environment and Climate Change Canada, Toronto, Ontario, Canada}

Correspondence to: J. Burkart (jburkart@chem.utoronto.ca)

Abstract

Motivated by increasing levels of open ocean in the Arctic summer and the lack of prior altitude-resolved studies, extensive aerosol measurements were made during 11 flights of the NETCARE July 2014 airborne campaign from Resolute Bay, Nunavut. Flights included vertical

profiles (60 to 3000 m above ground level) over open ocean, fast ice, and boundary layer clouds and fogs. A general conclusion, from observations of particle numbers between 5 and 20 nm in diameter (N_{5-20}), is that ultrafine particle formation occurs readily in the Canadian high Arctic marine boundary layer, especially just above ocean and clouds, reaching values of a few thousand particles/cm^3. By contrast ultrafine particle concentrations are very much lower in the free troposphere. Elevated levels of larger particles (for example, from 20 to 40 nm in size, N_{20-40}) are sometimes associated with high N_{5-20}, especially over low clouds, suggestive of aerosol growth. The number densities of particles greater than 40 nm in diameter ($N_{>40}$) are relatively depleted at the lowest altitudes, indicative of depositional processes that will lower the condensation sink and promote new particle formation. The number of cloud condensation nuclei (CCN, measured at 0.6% supersaturation) are positively correlated with the numbers of small particles (down to roughly 30 nm), indicating that some fraction of these newly formed particles are capable of being involved in cloud activation. Given that the summertime marine Arctic is a biologically active region, it is important to better establish the links between emissions from the ocean and the formation and growth of ultrafine particles within this rapidly changing environment.

1 Introduction

Surface temperatures within the Arctic are rising almost twice as fast as in any other region of the world. As a manifestation of this rapid change the summer sea ice extent has been retreating dramatically over the past decades with the possibility that the Arctic might be ice free by the end of this century (Boé et al., 2009) or even earlier (Wang and Overland, 2012). Arctic aerosol is well known to show a distinct seasonal variation with maximum mass concentrations and a strong long-range anthropogenic influence in winter and early spring. The phenomenon, known as Arctic Haze, was identified many years ago (e.g. Barrie, 1986; Heintzenberg, 1980; Rahn et al., 1977; Shaw, 1995), and has commanded renewed attention in recent years (e.g. Law et al., 2014; Quinn et al., 2007). During summer the Arctic is more isolated from remote anthropogenic sources and represents a comparatively pristine environment. The reason is that the Arctic front (e.g. Barrie, 1986), which provides a meteorological barrier for lower-level air mass exchange,

moves north of many source regions during the summer months. Anthropogenic and biomass burning aerosols are transported to the Arctic during the summer, but increased aerosol scavenging helps maintain the pristine conditions near the surface (e.g. Browse et al., 2012; Croft et al., 2016a; Garrett et al., 2011).

Zhang et al. (2010) discuss the impacts of declining sea ice on the marine planktonic ecosystem, which includes increasing emissions of dimethyl sulfide (DMS) that may contribute to particle formation in the atmosphere (e.g. Charlson et al., 1987; Pirjola et al., 2000). Enhanced secondary organic aerosol from emissions of biogenic volatile organic compounds is also a possibility (Fu et al., 2009). Primary emissions of aerosol particles from the ocean, such as sea salt and marine primary organic aerosol, may also increase (Browse et al., 2014). Open water tends to increase cloudiness, which means that aerosol influences on clouds are likely to be more important. Over the Arctic the effects of aerosols on clouds are especially uncertain. Models have predicted that increasing numbers of particles may lead to overall warming (Garrett, 2004) when the atmosphere exists in a particularly low particle number state now referred to being "CCN limited" (Mauritsen et al., 2011), to an overall cooling effect when increasing numbers of particles are added to an atmosphere with more particles already present (Lohmann and Feichter, 2005; Twomey, 1974). It is important to characterize particle size distributions in this pristine environment to provide a baseline against which future measurements can be compared in a warming world. Indeed, Carslaw et al. (2013) highlight the need to understand pre-industrial-like environments with only natural aerosols in order to reduce the uncertainty in estimations of the anthropogenic aerosol radiative forcing.

Primary sources, gas-to-particle formation processes, cloud processing, atmospheric aging, mixing and deposition are all reflected in the size distribution. Therefore, measurements of aerosol size distributions are important for understanding the processes particles undergo in addition to their potential effects on clouds. The presence of ultrafine particles indicates recent production as their lifetime is on the order of hours. We focus this paper on ultrafine particles as these are an indication for in-situ aerosol production processes in the Arctic. We also consider the growth of newly formed particles, as that determines how important they are for climate.

Aerosol size distributions including ultrafine particles (dp < 20 nm) have been measured before at different locations throughout the Arctic. Long term studies at ground stations such as Alert, Nunavut (Leaitch et al., 2013), Ny Alesund and Zeppelin (Engvall et al., 2007; Ström et al., 2003, 2009; Tunved et al., 2013), both on Svalbard and very recently in Tiksi, Russia (Asmi et al., 2016) and Station Nord, Greenland (Nguyen et al., 2016) indicate a strong seasonal dependence of the size distribution with the accumulation mode aerosol dominating during the winter months and a shift to smaller particles during the summer months. New particle formation events are frequently observed from June to August. Ström et al. (2003) show that the size distribution undergoes a rapid change from an accumulation mode dominated distribution during the winter months to an Aitken mode dominated distribution at the beginning of summer. Total number concentrations increase at the beginning of summer and roughly follow the incoming solar radiation on a seasonal scale suggesting that photochemistry is an important factor for new particle formation in the Arctic. At Ny Alesund maximum number concentrations occur in late summer and are explained by the Siberian tundra being a potential source of aerosol precursor gases (Ström et al., 2003) and marine biogenic sulphur (Heintzenberg and Leck, 1994). Analysis of air mass patterns for this region show that the shift in the size distributions is also accompanied by a change of source areas, with a dominance of Eurasian source areas in winter and North Atlantic air during summer (Tunved et al., 2013).

Particle measurements including aerosol size distributions were also conducted from ice breaker cruises such as from the Swedish ice breaker Oden (Bigg and Leck, 2001; Covert et al., 1996; Heintzenberg and Leck, 2012; Leck and Bigg, 2005; Tjernström et al., 2014) and the Canadian Coast Guard Ship ice breaker Amundsen (e.g. Chang et al., 2011). Chang et al. (2011) used model calculations to show that the appearance of ultrafine particles can be explained by nucleation and growth attributed to the presence of high atmospheric and oceanic DMS concentrations measured at the same time. The Oden expeditions focus on the pack-ice-covered high Arctic, mainly north of 80N and also confirm the frequent presence of an UFP mode (e.g. Covert et al., 1996). The observations from the Oden cruises offer evidence that UFP in the inner Arctic might originate from primary sources (e.g. Heintzenberg et al., 2015; Karl et al., 2013). This is motivated by three main observations. First, a lack of sulfuric acid components in collected 15-50 nm particles (Leck and Bigg, 1999). Second, Leck and Bigg (2010) highlight

112 that nucleation events in the high Arctic do not follow the classical banana shaped growth curve
113 (Kulmala et al., 2001) but enhanced levels of ultrafine particles rather appear simultaneously in
114 distinct size ranges (Karl et al., 2012). Third, such events could not be modelled with the selected
115 empirical nucleation mechanism for the extremely low DMS concentrations in this region (Karl
116 et al., 2013). As a primary source marine microgels are suggested that might become airborne via
117 the evaporation of fog and cloud droplets (Heintzenberg et al., 2006; Karl et al., 2013).

118 So far most studies that include size distribution measurements in the summertime Arctic were
119 conducted from ground stations or ship cruises. To date there are only two studies that assess the
120 altitude dependence of the size distribution:, i.e. one in the area of Svalbard (Engvall et al., 2008)
121 and one from the Oden performing vertical profiles with a helicopter (Kupiszewski et al., 2013).
122 Although no size distribution measurements were performed, Heintzenberg et al. (1991)
123 measured vertical profiles of the total particle number concentration greater than 10 nm during
124 June and July, 1984 over the Fram Strait-Spitsbergen area, and found a "rather uniform
125 distribution" with altitude. Their measurements, however, were confined to 500 m-MSL and
126 above.

127 In this study we present data from aerosol size distribution measurements taken from an aircraft
128 during a three week period in July 2014 in the high Arctic area of Resolute Bay, Nunavut,
129 Canada. The flights focused on vertical profiles from as low as 60 m above the ground up to
130 3km, as well as on low-level flights above different terrain such as fast ice, open ocean, polynyas
131 and clouds. We focus especially on UFP (5-20 nm in diameter) and address the following
132 questions: What are the concentrations of UFPs in the Arctic summertime, and what is their
133 vertical distribution? What are the environmental conditions that favour occurrence of UFPs?
134 And, is there evidence for growth of UFP to CCN sizes? Aside from the studies conducted near
135 Svalbard, we believe this is the first aircraft study in the high Arctic to systematically address
136 these specific questions. This work provides a comprehensive picture of UFPs observed during
137 the campaign whereas a prior publication from Willis et al., (2016) detailed one UFP formation
138 and growth event observed over Lancaster Sound.

139

2 Experimental

2.1 Sampling Platform Polar 6

The research aircraft Polar 6 owned by the Alfred Wegener Institute, Helmholtz Center for Polar and Marine Research, Bremerhaven, Germany served as the sampling platform. The Polar 6 is a converted DC-3 airplane (Basler BT-67) modified to work under extreme cold weather conditions. An advantage of the plane is that flights at very relatively low speeds and altitudes (< 60 m a.g.l.) are possible. The cabin of the aircraft is non-pressurized. We maintained a constant survey speed of approximately 120 knots (222 km h^{-1}) for measurement flights at constant altitude, and ascent and descent rates of 150 m min^{-1} for vertical profiles. Instruments and measurements specific to this paper are described below.

2.1.1 Inlets

Aerosol was sampled through a stainless steel inlet mounted to the top of the plane and ahead of the engines to exclude contamination. The tip of the inlet consisted of a shrouded diffuser that provided nearly isokinetic flow. Inside the cabin the intake tubing was connected to a stainless steel tube (outer diameter of 2.5 cm, inner diameter of 2.3 cm) that carried the aerosol to the back of the aircraft where it was allowed to freely exhaust into the cabin so that the system was not over-pressured. The stainless steel tube functioned as a manifold, off which angled inserts were used to connect sample lines to the various instruments described below. In-flight air was pushed through the line with a flow rate of approximately 55 L min^{-1} determined by the sum of the flows drawn by the instruments (35 L min^{-1}), plus the flow measured at the exhaust of the sampling manifold (20 L min^{-1}). A flow of 55 L min^{-1} was estimated to meet nearly isokinetic sampling criteria at survey speed and the transmission of particles through the main inlet was approximately unity for diameters between 20 nm to 1 μm (Leaitch et al., 2016). Although the transfer of the aerosol from outside to the instruments is relatively fast (5 seconds or less), volatilization of some components of the particles may have occurred. However, the growth of newly formed particles by organic condensation occurs primarily by low volatility organic components (e.g. Pierce et al., 2012). Thus, the integrity of the smaller particles is likely to have

been maintained. We do expect increasing line losses of particles with sizes decreasing from 10 nm. Therefore our observations will underestimate N_{5-20}.

Trace gases (CO and H_2O) were sampled through a separate inlet made of a 0.4 cm (outer diameter) Teflon tube entering the aircraft at the main inlet and exiting through a rear-facing 0.95 cm exhaust line that provided a lower line pressure. The sample flow of approximately 12 L min^{-1} was continuously monitored.

2.2 Instrumentation

2.2.1 Meteorological parameters and state parameters

Aircraft state parameters and meteorological measurements were performed with an AIMMS-20 manufactured by Aventech Research Inc. at a very high sampling frequency (>40Hz). The AIMMS-20 consists of three modules: (1) The Air Data Probe that measures the three-dimensional aircraft-relative flow vector (true air speed, angle-of-attack, and sideslip), and turbulence with a three-dimensional accelerometer. As well, temperature and humidity sensors are contained within this unit and provide an accuracy and resolution of 0.30 and 0.01 C for temperature and 2.0 and 0.1% for relative humidity measurements. (2) An Inertial Measurement Unit that consists of three gyros and three accelerometers providing the aircraft angular rate and acceleration; (4) A Global Positioning System for aircraft 3D position and inertial velocity. Horizontal and vertical wind speeds were measured with accuracies of 0.50 and 0.75 m s^{-1}, respectively. The high frequency raw data were processed to 1Hz resolution. Further details of the AIMMS including data processing can be found in (Aliabadi et al., 2016a).

2.2.2 Aerosol physical and chemical properties

Particle number concentrations and particle size distributions were measured with a TSI 3787 water-based ultrafine Condensation Particle Counter (UCPC), a Droplet Measurement Technology (DMT) Ultra High Sensitivity Aerosol Spectrometer (UHSAS) and a Brechtel Manufacturing Incorporated (BMI) Scanning Mobility System (SMS) coupled with a TSI 3010 Condensation Particle Counter (CPC). The UCPC detected particle concentrations of particles larger than 5nm in diameter with a time resolution of 1 Hz. The flow rate was set to 0.6 L min^{-1}.

194 The particle concentrations measured by the UCPC are referred to as N_{tot} hereafter, noting as
195 above that diffusional losses of particles smaller than 10 nm make the N_{tot} observations lower
196 limits.

197 The BMI SMS was set to measure particle size distributions from 20nm to 100nm with a sample
198 flow of 1 L min^{-1} and a sheath flow of 6 L min^{-1}. The duration of one scan was 40 s with a 20 s
199 delay time before each scan resulting in a time resolution of 1min. The UHSAS performed size
200 distribution measurements from 70 nm – 1 µm at a time resolution of 1 Hz with a sample flow
201 rate of 55 cm^3 min^{-1}. Details of the calibrations and instrument inter-comparisons performed
202 prior and during the campaign are described in detail in Leaitch et al. (2016).

203 Cloud condensation nuclei (CCN) were measured with a DMT CCN Counter (CCNC). The
204 CCNC was operated behind a constant pressure inlet that was set to 650 hPa. The nominal
205 supersaturation was held constant at 1%. Calibrations prior and during the campaign (for details
206 see Leaitch et al. 2016) showed that a nominal supersaturation of 1% at the reduced pressure
207 translated into 0.6% effective supersaturation.

208 Cloud droplet sizes from 2-45 µm were measured using a wing mounted Particle Measuring
209 System (PMS) FSSP 100. In this study these data are only used to identify periods when the
210 aircraft was flying in cloud. To avoid possible artefacts produced from shattering of cloud
211 droplets at the aerosol inlet, data from in-cloud times are discarded for the purposes of this study.

212 A DMT Single Particle Soot Photometer (SP2) was deployed to measure refractory black carbon
213 (rBC) number and mass concentrations. We refer to rBC mass concentrations as an indication of
214 pollution influence. Calibrations with Aquadag soot were performed prior to and during the
215 campaign. The lower size limit of detection of rBC particles by the SP2 was approximately
216 80nm.

217 Sub-micron aerosol composition was measured with an Aerodyne high-resolution time-of-flight
218 aerosol mass spectrometer (HR-ToF-AMS; e.g. DeCarlo et al., 2006). A detailed description of
219 the instrument is found in Willis et al. 2016. The main purpose of the instrument was to measure
220 non-refractory particulate matter such as sulfate, nitrate, ammonium, methane sulfonic acid

(MSA) and the sum of organics. Detection limits were 0.009, 0.008, 0.004, 0.005 and 0.08 µg m^{-3}, respectively, for a 30 second averaging time.

2.2.3 Trace gases

Carbon monoxide (CO) was measured with an Aerolaser ultra-fast carbon monoxide monitor model AL 5002 based on VUV fluorimetry, employing the excitation of CO at 150 nm. In-situ calibrations were performed during flight at regular intervals (15 – 30 min) using a NIST traceable CO standard with zero water vapor concentration. CO mixing ratios were used as a relative indicator of aerosol influenced by pollution sources.

Water vapour (H_2O) measurements were based on infrared absorption using a LI-7200 enclosed CO_2/H_2O Analyzer from LI-COR Biosciences GmbH. The measurement uncertainty is ± 15 ppm_v. H_2O mixing ratios were used to calculate relative humidity with pressure and temperature measured by the AIMMS-20.

2.3 Data analysis and nomenclature of particle size data

All particle data were averaged to 1 min intervals to match the time resolution of the BMI SMS. Particle concentrations within different size intervals were calculated. The notation N_{a-b} is used; "a" gives the lower limit and "b" the upper limit of the calculated size interval. The BMI SMS was used to determine concentrations of particles from 20-90 nm diameter, and concentrations of particles larger than 90 nm diameter were determined by the UHSAS. If the size interval is expressed as $N_{>a}$ the upper limit is given by the detection limit of the UHSAS (1µm). Additionally, particle concentrations from 5-20 nm (short: N_{5-20}) were obtained by subtracting particle concentrations measured by the BMI SMS and by the UHSAS from the N_{tot} as determined by the CPC. The N_{5-20} are also referred to as ultrafine particles (UFP) in this study.

In order to obtain vertical profiles the data were averaged within altitude intervals. An average profile for a single flight was obtained by binning all data from the respective flight into altitude intervals of 100m starting at the lowest flight altitude. In addition to data obtained during vertical profile flights, data aquired while flying at a constant level were also included. Average profiles

containing data from more than one flight were calculated by averaging the respective single flight profiles.

Average size distributions were obtained by simply averaging each bin for the desired time and altitude range. The size distributions measured by the BMI SMS were used for particle sizes from 20-90 nm, and the distributions at larger sizes are taken from the UHSAS. All particle concentrations are expressed for ambient pressure conditions, i.e. they have not been adjusted to standard temperature and pressure conditions. The $N_{5\text{-}20}$ referred to as UFP are added to the size distributions as additional bin assuming a bin width of 15 nm (from 5-20 nm) with the mid diameter of 12nm.

2.4 FLEXPART-WRF Simulations

We used FLEXPART-WRF (Brioude et al., 2013, website: flexpart.eu/wiki/FpLimitedareaWrf) simulations run backwards in time to analyse the origins of air masses sampled along the flight tracks. FLEXPART-WRF is a Lagrangian particle dispersion model based on FLEXPART (Stohl et al., 2005). Meteorological information is obtained from the Weather Research and Forecasting (WRF) Model (Skamarock et al., 2005). FLEXPART-WRF outputs retroplume information such as the residence time of air (over a unit area) prior to sampling. Residence times were integrated over the entire atmospheric column and 7 days backward in time. FLEXPART-WRF was run in two ways. First, one FLEXPART-WRF was completed for each flight using particle releases every 2 minutes along the flight track (100 m x 100 m x 100 m centered on the aircraft location) to produce potential emissions sensitivities (PES) that represent the average airmass origin for each flight. Second, separate runs were completed for points (every 10 minutes) along the flight track (100 m x 100 m x 100 m, 60 second release duration) in order to study different airmasses measured during the same flight. A more detailed description of the model as used for NETCARE 2014 is provided by Wentworth et al. (2015).

2.5 Study area and flight tracks

From July 4th to July 21st, 2014 eleven flights were conducted out of Resolute Bay (74.7 N, 95.0 W). In Figure 1 a compilation of all flight tracks on a satellite image is shown. The satellite picture was taken on July 4th, 2014 and reflects the situation of the region during period I (July 4 to July 12). Resolute Bay proved to be an ideal location for this study as we had access to both open ocean and ice covered regions. Additionally two polynyas were located north of Resolute Bay within the reach of our aircraft. Flights ranged between 4-6 hours. The flights covered two main areas: Lancaster Sound east of Resolute Bay and the area north of Resolute Bay where two polynyas were located. The flights south of Resolute Bay in Lancaster Sound concentrated around the ice edge.

The ice/water coverage visible on the satellite picture is representative for the area during the first period. As can be seen, the ice edge was situated about 150 km east of Resolute Bay. It is clearly visible in the satellite image as a sharp line. The transition from a completely ice covered region to open ocean was very abrupt during the first period. Only after a period of bad weather with high winds did the ice edge become less clear, and the region starting about 80 km east of Resolute Bay to about 200 km east was covered by fractured ice.

Roughly 50% of the flight time was within the inversion layer, and 50% was in the free troposphere conducting altitude profile flights. A considerable amount of time was spent at 2800 m as this was the preferred altitude when travelling to a certain area. When clouds were present, the aircraft sampled them by slant profiling through the cloud in the case clouds were above the boundary layer, or, in the case clouds were within 200 m of the surface, by descending into the cloud as low as possible. Aerosol observations while inside cloud are excluded from the analysis here due to potential artifacts from droplets shattering on the outside inlet.

3 Meteorological and atmospheric conditions

Meteorological conditions changed over the course of the campaign. Similar conditions were encountered during the first part of the campaign (July 4th – July 12th, 6 flights), referred to as the "Arctic air mass period" because air masses from within the Arctic dominated and the

atmosphere showed structures typical for the Arctic such as a low boundary layer height with thermally stable conditions, indicated by a near surface temperature inversion, and frequent formation of low level clouds. At this time Resolute Bay was under the influence of high pressure systems. Clear sky with few or scattered clouds and low wind speeds dominated. Conditions changed starting from July 13th when the region was influenced by troughs of a low pressure system located to the west above Beaufort Sea, which eventually passed through Resolute Bay on July 15th bringing along humidity, precipitation and fog. Intense fog and low visibility impeded flying from July 13th to July 16th. A short good weather window in which the fog dissipated permitted flying again on July 17th (referred to as "transition day"; one flight) just before Resolute Bay came under influence of a pronounced low pressure system located to the south with its center around King William Island (69.0 N, 97.6 W). The last campaign days (referred to as "southern air mass period", three flights) were characterised by the influence of this pronounced low pressure system bringing air masses from the south and providing higher wind speeds, an overcast sky and occasional precipitation.

Vertical profiles of median temperature, relative humidity (RH), wind speed, CO and N_{tot} (Figure 2) illustrate median atmospheric conditions during the measurement flights. Prominent features representing the trend of each period and reflecting the general meteorological situation will be described here, with details discussed in the respective sections. The Arctic air mass period was characterized by frequent thermally stable conditions within the near surface layer , representing typical conditions during the Arctic summertime (Aliabadi et al., 2016a; Tjernström et al., 2012). The median temperature profiles show that on average the boundary layer reached up to ~300 m with a temperature increase of about 5 C. In this paper we will refer to this part of the atmosphere as the boundary layer (BL) and to the air masses above as the free troposphere (FT). A BL height of 300m corresponds well to the boundary layer height of 275 +/- 164 m estimated by (Aliabadi et al., 2016a) using the method of bulk Richardson number (Aliabadi et al., 2016b) and a critical bulk Richardson number of 0.5, using data from radiosondes launched at Resolute Bay and the Amundsen icebreaker, which also performed research operations in Lancaster sound during the campaign period.

Within the BL particle concentrations spanned over a wide range of concentrations (max N_{tot}: ~10000; median values: ~150 to ~1700 cm^{-3}). Highest N_{tot} occurred during the Arctic air mass period, while N_{tot} was constantly low within the lower atmosphere on the transition day. Median temperatures near the surface ranged from -1 C to 5 C during the Arctic air mass period, largely depending on the terrain below (e.g. ice or open water) and were clearly higher during when the southern air masses arrived (e.g. at the "surface": 4 C and 7 C, respectively) and, if present, the BL was less pronounced. The higher temperatures coincide with the influence of low pressure systems bringing warmer air masses from the west and south and additional higher wind speeds providing a better mixing of the atmospheric layers (5.6 ms^{-1} vs $12m^{-1}$ near the surface). CO mixing ratios were extremely low during the Arctic air mass period (median: 78.3 ppb_v) and on the transition day (median: 83.4 ppb_v) indicating pristine air masses that had not recently been affected by pollution or biomass burning sources. During the southern air mass influence CO mixing ratios clearly increased (median: 95.0 ppb_v) confirming a change in air mass and suggesting possible influences by pollution sources and wild fires in the North West Territories (Supplementary Figure 2). Relative humidity profiles show that the near surface layer of the atmosphere was very moist with RH > 80 % during all periods.

4 Results and Discussion

4.1 Ultrafine particle events

4.1.1 Frequency of ultrafine particle events

Throughout the campaign we observed large variability in particle concentrations (Figure 3). We observed not only very clean air masses with N_{tot} of a few tens cm^{-3} (with the lowest 1-second value of 1 cm^{-3}), but also concentrations as high as a few thousands per cm^{-3} (with the highest value of 10000 cm^{-3}). The highest and lowest concentrations were measured within the BL (Figure 3b). Above the BL (Figure 3b) particle concentrations were relatively constant where 60% of the time concentrations were between 200 - 300 cm^{-3} (for a discussion of the average size distribution see sections 4.1.2 - 4.1.4). Especially during the Arctic air mass period (Figure 2) the atmosphere was characterized by a strong contrast between the BL and the FT.

UFP were very frequently present within the BL in high concentrations (Figure 3c). Here we refer to "bursts" of particles as a sudden and relatively large increase in N_{5-20}: concentrations suddenly rising from tens cm^{-3} to several hundreds and thousands cm^{-3}. This may reflect inhomogeneities in the NPF process or reflect the aircraft flying in and out of areas of high UFP concentrations. Bursts of $N_{5-20} > 2000/cm^3$ were observed over polynyas, consistent with previous observations (Leaitch et al., 1984; 1994), in Lancaster Sound and south of Resolute Bay. The N_{5-20} was higher than 200 cm^{-3} during 65% of the time. Indeed, high N_{tot} was mainly driven by UFP (as can be seen by comparison of black dots indicating high N_{tot} in Figure 3c and high UFP in Figure 3d). Whenever N_{tot} is greater than 2000 cm^{-3}, UFP was larger than 1000 cm^{-3}. This is also illustrated by the ratio of UFP/N_{tot} (Figure 3e). A ratio of zero means that no UFP were present, while a ratio of one means that only UFP were present. Within the boundary layer 32% of the time the size distribution was dominated by UFP (ratio > 0.5).

The frequent presence of UFP agrees well with other studies made during the Arctic summertime at several locations, such as at the ground stations in Ny Alesund and Zeppelin (Ström et al., 2009; Tunved et al., 2013), at Alert (Leaitch et al., 2013), and from ship-based observations (Chang et al., 2011; Covert et al., 1996; Heintzenberg et al., 2006). However, such a frequent presence of an UFP mode (65% of the time > 200 cm^{-3}) in the BL is unique to this study. Possible reasons for the higher occurrence of UFP might be the combination of the proximity of open ocean (providing a source of UFP or precursor gases), favourable meteorological conditions (sunny weather, inversion layer with cloud formation) and very clean air masses with low condensation sinks. Also, since observations of UFP were one focus of this study, the fractional occurrence of the UFP mode may be biased slightly high due to longer sampling times associated with UFP occurrence. Calm weather conditions may have been another factor. The highest concentrations of UFP were measured at lower wind speeds (< 5m s^{-1}; Supplementary Figure 1), while lower UFP concentrations (1000 cm^{-3}) were found at higher wind speeds (>12ms^{-1}) suggesting a dilution effect of the wind. Such a dilution effect implies proximity to the source.

386 In the following sections, the vertical distribution of UFP and the size distributions are discussed
387 in relation to meteorological conditions during the three distinct periods that characterized this
388 campaign.

389

390 ### 4.1.2 Arctic air mass period: July 4th to July 12th

391 During this first period the study area was under the influence of a high pressure system. As
392 illustrated by FLEXPART-WRF results (Figure 4a and 4b), air masses were either coming from
393 the North extending to the east in the Arctic Ocean or from the East passing over the open ocean
394 in Lancaster Sound and Baffin Bay. Both examples indicate that air masses resided within the
395 Arctic region at least 5 days prior to sampling. This is true for all flights during this period. The
396 very low CO mixing ratios (78 ppb_v, see Figure 2) and average BC mass concentrations of 3 ng
397 m^{-3} (not shown) confirm that air masses were very clean and without recent influence from
398 pollution sources. As discussed in section 3, temperature profiles indicate thermally stable
399 conditions in the lowest layers with near-surface temperature inversions. During almost all
400 vertical profiles we observed temperature inversions of about 4-6 C near the surface. Such an
401 atmospheric structure i.e. a shallow boundary layer is typical for the Arctic summertime (e.g.
402 Aliabadi et al., 2016a; Tjernström et al., 2012).

403 The Arctic air mass period was characterized by a very sharp contrast between the BL and the
404 FT in terms of particle number concentrations and sizes (Figure 5). The BL was characterized by
405 a prominent layer of UFP from the surface to about 300 m with the highest concentrations closest
406 to the surface (Figure 5a). The height of the UFP layer coincides with the average height of the
407 temperature inversion for this period (see temperature profile Figure 2) and indicates that air
408 masses were stably layered limiting exchange with the FT. This is supported by the observed
409 lower turbulent mixing (i.e. turbulent kinetic energy) from boundary layer to the free troposphere
410 during the campaign (Aliabadi et al., 2016a).

411 During this period we measured the highest concentrations of UFPs with the one minute average
412 up to 5300 cm^{-3}. On a typical flight several bursts (see Section 4.1.1) of high UFP concentrations
413 were encountered in the BL. Particle bursts lasted from a few seconds to several minutes,

corresponding to a spatial extent of several hundreds of meters to dozens of kilometers. The large spatial variability is also illustrated by the frequency distribution of UFP in the BL shown in Figure 5c: 40% of the time concentrations of UFP were larger than 200 cm^{-3}, 11% of the time larger than 1000 cm^{-3} and 3% of the time even larger than 2000 cm^{-3}. Particle concentrations in the FT are relatively uniform, and concentrations of UFP were less than 50 cm^{-3} up to 1200m and ~10 cm^{-3} above.

The average N_{20-40} is similar to the UFP, showing a maximum in its concentration at the same altitude. The concentrations of larger particles ($N_{>40}$, $N_{>80}$, $N_{>150}$) are much lower in the clean BL (surface areas of ~5μm^2 m^{-3} and lower). However, the $N_{>40}$ and $N_{>80}$ increase from the lowest altitude to the next averaged altitude, consistent with the increase in the UFP and N_{20-40}. These results suggest that some of the UFP experienced growth to sizes of 20-80 nm within a few hours, as demonstrated by Willis et al. (2016). Within the FT particle concentrations were surprisingly uniform and concentrations of UFP were less than 50 cm^{-3} up to 1200m and ~10 cm^{-3} above.

In Figure 5b, the median size distribution shows that increases in UPF in the BL were frequent. The average size distribution shows that at times higher concentrations of particles extended up to about 80 nm, consistent with the suggestion above that some UFP particles experienced growth to larger sizes. A relevant case will be discussed in Section 4.3. Occasionally a mode of particles larger than 400 nm was present in the BL over open water (see Section 4.2), which was likely the product of primary oceanic emissions.

4.1.3 Transition day on July 17th

July 17th marks the transition from dominance by Arctic air masses to a more distant influence from southern air masses. The transition day consists of only one flight in the area of Lancaster Sound, during which low concentrations of particles larger than 20 nm were observed below 600 m: e.g. $N_{>40}$ ranged from 60 cm^{-3} to 100 cm^{-3}; see Figure 6. The deeper layer of lower concentrations may have been a result of cloud processing and scavenging. During the days before flying was impossible because of intense fog and cloud at Resolute Bay. A different

transport regime may also have contributed to this situation. On this day the low pressure system situated to the west was bringing air masses from the west along the Canadian and Alaskan coastline (Figure 4c). The temperature profile shows an inversion between 650-1000m possibly indicating a change in air mass. CO mixing ratios (83ppb$_v$) and BC mass concentrations (3ng/cm^{-3}) were also quite low indicating mostly Arctic background conditions.

On this day, occasional bursts of UFP up to 1400-1900 cm^{-3} were observed within the bounday layer (Figure 6b). UFP of 200 cm^{-3} or more were observed about 20% of the time (Figure 6c), and the average concentration was 240 cm^{-3} at the lowest level of the profile (Fig. 6a). Concentrations of larger particles ($N_{>40}$, $N_{>80}$, $N_{>150}$) increased sharply at about 700m coinciding with the temperature inversion. The very low concentrations of larger particles ($N_{>150}$: <10 cm^{-3}) below the temperature inversion are very similar to the conditions encountered within the BL during the previous period. As above, the differences in the transition day below 700 m may have been due to a combination of fog/cloud scavenging and a change of air mass. Median and average size distributions indicate a minimum at around 65nm that might be the result of cloud processing (Hoppel et al., 1994), consistent with the Arctic observations of (Heintzenberg et al., 2006) and the activation diameters observed during this study (Leaitch et al., 2016).

4.1.4 Southern air mass period: July 19th – July 21st

During this period the region was under the influence of a low pressure system centered south of Resolute Bay. FLEXPART-WRF air mass trajectories (Figures 4d and 4e) indicate a prevalence of air masses from the south potentially affected by wild fires (see Supplementary Figure 2). At the beginning of this period on July 19th (Figure 4d), air mass trajectories suggest the strongest influence from the south while towards the end of the period on July 21st (Figure 4e), FLEXPART-WRF indicates that southern air masses mixed with air masses coming off Greenland. Near surface temperatures were higher than during the previous periods (Figure 2) and temperature inversions were less pronounced (2-4 C) and not observed at all locations suggesting a less stable lower atmosphere. On July 19th we encountered the highest wind speeds in the BL (16 m/s within the near surface layer and 20 m/s slightly above). Also RH was relatively high near the surface (91%) and did not drop below 80% throughout the vertical

atmosphere. CO mixing ratios were higher than during the prior periods suggesting that the air was at times influenced by pollution or biomass burning.

UFP were observed less frequently than during the Arctic air mass period and in lower concentrations (Figure 7). Bursts of UFP above 1000 cm^{-3} occurred only at three locations, all during the flight on July 21st. Average UFP concentrations were only approximately 190 cm^{-3}. UFP concentrations of 200 cm^{-3} or higher were detected 31% of the time below 300m (Figure 7c).

The southern air mass period clearly shows different aerosol characteristics within the near surface layer than compared to the Arctic air mass period and the transition day. Average concentrations of particles larger than 40 nm were highest within the boundary layer and decreased with altitude (Figure 7a). This is in sharp contrast to the cleaner boundary layers observed before. Whereas concentrations of particles larger 40nm were ~100 cm^{-3} and lower during both prior periods, they were as high as 300 cm^{-3} for this period. Even large accumulation mode particles ($N_{>150}$) averaged ~50 cm^{-3} (compared to 10 cm^{-3} for both previous periods). Also, both the median and average size distributions show a pronounced mode of particles larger than 500 nm within the BL (Figure 7b). Primary emissions from the sea spray promoted by the higher surface wind speeds (see Figure 2) are likely a factor contributing to the larger particles.

During the southern air mass period, three important factors had changed compared to both prior periods. (1) Air mass back trajectories had clearly shifted to the south and potentially transported emissions from wild fires located in the Northwest Territories (Supplementary Figure 2) into the region, which might mix into the boundary layer. (2) The Amundsen ice breaker was present in Lancaster Sound and acted as a local pollution source. (3) Wind speeds were higher and the ocean was visibly turbulent with breaking waves that might enhance primary oceanic aerosol emissions. The increased condensation sinks from these potential sources in combination with other factors (e.g. reduced sun light) and relatively low residence times of air masses within the boundary layer (compared to the Arctic air mass period) may explain the relatively low and infrequent concentrations of UFPs.

Within the FT the size distributions shows a bimodal character with a minima at 60-80 nm, which may indicate the air masses experienced cloud processing. This is likely, given the

499 presence of the low pressure system bringing moister and warmer air masses. The bimodal size
500 distribution is different from the average size distribution during the Arctic air mass period when
501 drier air masses from within the Arctic dominated.

502 4.2 UFP occurrence above ice versus water

503 We investigated the potential influence of different underlying water surfaces on the occurrence
504 of UFP by examining in detail the time periods when we were flying at altitudes at or below 500
505 m during the Arctic air mass period. We distinguish between three water surfaces: ice covered
506 areas (including ice edge and ice covered with melt ponds), open ocean (including polynyas),
507 and low-level clouds (including both cloud above water and cloud above ice). Here we point out
508 that the case "cloud" does not include in-cloud flight times but only flight periods when above
509 cloud top without actually entering the cloud (confirmed by a zero signal in a liquid cloud probe
510 (FSSP100)). An altitude of 500 m was chosen to include time periods when we were flying
511 above low-level clouds and to capture mostly flights within the boundary layer where a local
512 influence of the terrain below was likely. During the Arctic air mass period, there was a clear
513 separation between ice and open water over Lancaster Sound with east of the ice edge
514 completely ice free, while west of the ice edge the ocean was seamlessly covered by fast ice (see
515 satellite picture in Figure 1).

516 Each average profile above the different water surface exhibits unique features (Figure 8). Above
517 ice the highest concentrations of UFP (average: 400 cm^{-3}) were found nearer the surface (70 m)
518 and the N_{tot} are slightly higher (580). In the BL over open water, the N_{tot} and UFP number
519 concentrations are 900 cm^{-3} and 560 cm^{-3}, respectively, and in the air just above cloud, the
520 average N_{tot} and UFP number concentrations are 2000 cm^{-3} and 1040 cm^{-3}, respectively. In the
521 open water and cloud cases, the highest concentrations of ultrafines are at the point of
522 measurement closest to the water surface. In the cloud case and open water case, the N_{20-40}
523 particles show an increase at the same time as the N_{tot} and UFP suggesting that the UFP form and
524 grow to larger sizes. This is not observed in the over-ice case, which suggests that some of the
525 new particles could have formed elsewhere (e.g. over open water) and been transported over the
526 ice, or that the growth rates over ice are slow. In all three cases, the largest particles show

relatively smaller abundances at the lowest altitudes samples. An increased abundance of UFP at lower surface areas supports the hypothesis that UFP form via nucleation of precursor gases.

4.3 Case study: July 8

The flight on July 8 provides a case study illustrating that the occurrence of UFP is confined to the BL suggesting a surface source of UFP and that the appearance of UFP is promoted by cloud. We consider the altitude dependence of the UFP within the BL in relation to air mass history and cloud.

On this flight we first flew out into Lancaster Sound west of Resolute Bay, turned around and descended into the BL above the ice. Here, we focus on the time period from 15:50 UTC (descent into the BL) to 17:20 UTC where we travelled from west to east and remained within the BL but stayed out of cloud as shown in Figure 9; see also Supplementary Figure 2. The later part of the flight focused on in-situ cloud properties and is discussed elsewhere (Leaitch et al., 2016). The weather was sunny with low level clouds starting around 150 km over ice and west of the ice edge in Lancaster Sound. The clouds had formed over the water and were blown over the ice where they were dissipating (Leaitch et al., 2016). In the entire area the atmosphere was characterized by a surface temperature inversion extending vertically up to about 300 m with ~1 C near the surface and ~5 C at 300 m and was accompanied by decreasing relative humidity (Figure 9f). Local low-level winds were predominantly from the south to east and wind speeds were below 5 ms^{-1}.

UFP were present throughout the BL with the highest concentrations at the lowest altitudes and decreasing concentrations towards the top of the BL (Figure 9b). In contrast, larger particles (e.g. $N_{>40}$) exhibit the opposite pattern, with lower concentrations at lower altitudes and higher concentrations at higher altitudes. Six locations from west to east (points A-F in Figure 9a) are used to illustrate the changing aerosol characteristics. Location A is situated well above the BL and at this point no UFP were present (detailed size distributions are shown in Supplementary Figure 4). At location B, the point at which we first entered the BL, an UFP mode (~370 cm^{-3}) was present at 60m, while UFP concentrations were lower at slightly higher altitudes (~80 cm^{-3} at 230 m) such as location C. At the lower altitudes the UFP concentrations gradually increased

555 as we approached the ice edge. The most striking observation is the steep increase in particle
556 concentrations at about 60 km west of the ice edge (location D) where UFP increased to above
557 4000 cm^{-3} at 150 m or just above cloud top. At the same time N_{20-40} concentrations showed a
558 similar increase. The increased UFP concentrations were vertically limited to near cloud top and
559 decreased rapidly with increasing altitude. The same pattern is also observed for temperature,
560 H_2O and CO_2 (Figure 9g) suggesting the existence of a distinct air mass at the surface that gets
561 diluted into the air mass above. Further east the flight was restricted to a slightly higher altitude
562 above cloud top. At point F, where we were close to the BL top, no peaks in particle
563 concentrations were observed. At point E, just before the ice edge, between the top of cloud and
564 the top of the BL, UFP concentations reached about 3400 cm^{-3}.

565 Air mass histories at these locations determined from FLEXPART-WRF (Figure 10) indicate the
566 following:
567 (1) To the west of Resolute Bay (point B) Lancaster Sound air masses had been mixed with air
568 masses from the North. This is also confirmed by the local wind directions indicating winds
569 coming from the Northwest sector (Figure 10a), and it is consistent with the associated change in
570 cloud. (2) Near the top of the BL, air masses had descended recently (< 3 h) into the BL (Figure
571 10c point C and point F). (3) In contrast, deeper within the BL at points B and D air masses had
572 descended into the BL earlier (~20 h) before arriving at the point of observation. In the case of
573 point D, where we observed the largest mode of UFP extending above 40nm, air masses had
574 been travelling from the east exclusively over the open waters in Lancaster Sound during the last
575 day before arriving at the point of observation.

576 Aerosol composition shows a clear difference between the aerosol in the FT and the BL. The
577 aerosol sulphate rapidly decreases as we enter the BL around 16:00, while aerosol organic mass
578 concentrations show an initial relative increase followed by an absolute increase towards the east
579 (Figure 9c). Within the BL aerosol organics and sulphate mass loadings show a pattern similar to
580 $N_{>40}$ and $N_{>80}$. Both decrease each time we descended deeper into the BL. However, at the same
581 time the organics-to-sulphate ratio indicates that the relative contribution of organics to aerosol
582 mass increases at lower altitudes and especially above cloud (Figure 9e). Well within the
583 inversion layer and in the vicinity of cloud top the aerosol was dominated by organics. At the

same time also ratio of MSA to sulphate was higher (Figure 9e), suggesting a marine biogenic influence of the aerosol sulphur. The marine biogenic influence at the lower altitudes agrees well with the FLEXPART-WRF simulations showing that air masses at this altitude had spent almost an entire day exposed to the open waters in Lancaster Sound. Consistent with the higher organic content measured with the AMS, the single particle aerosol mass spectrometer ALABAMA (Brands et al., 2011; Willis et al., 2016) detected a higher fraction of trimethylamine (TMA)-containing particles for particles larger than 150 nm in diameter (F. Köllner, personal communication, July 2016). Gaseous TMA emissions from marine biogenic origin (Ge et al., 2011; Gibb et al., 1999) may have additionally favored the subsequent growth of the freshly nucleated particles by condensation. Another possibility may be uptake of TMA in the cloud phase (Rehbein et al., 2011) if the particles have grown to sufficiently large sizes to be activated as CCN. Interestingly, compared to other days these TMA-containing particles are smaller and to a lesser degree internally mixed with potassium and levoglucosan which supports the hypothesis of ultrafine particles originating from nucleation in a biogenic marine environment and subsequent growth.

To explain these observations, we hypothesize that the smaller particle mode is formed by nucleation and growth occurring within the BL and especially in cloud vicinity. UFP concentrations near cloud top have been reported before (e.g. Radke and Hobbs 1991, Wiedensohler et al. 1997, Clarke et al., 1999; Garrett et al., 2002; Hegg et al., 1990; Mauldin et al., 1997) and it is suggested that nucleation in near cloud regions is favoured by the low surface areas, possibly due to cloud scavenged aerosol, moist air and a high actinic flux. Indeed, near cloud top where we observed an increase of UFP extending up to almost 50 nm the conditions for nucleation and growth are ideal. We speculate that the availability of precursor gases is provided by the long residence time (~20h) of the air masses over open water (Figure 10, point D). In other words, precipitating clouds scavenge aerosol particles, reducing the surface area for condensation, but some fraction of nucleation precursor gases with lower Henry's Law constants can pass through (e.g. SO_2) leaving the potential for H_2SO_4 in the higher OH in the cloud outflow (a discussion of the processes can be found in Seinfeld and Pandis, 1998). The very high organic loadings and MSA to sulphate ratio likely indicate that the formation and growth of these particles is driven by a combination of DMS and organic precursors (volatile organic

614 compounds) that are emitted by the open ocean in Lancaster Sound (e.g. Chang et al., 2011;
615 Sjostedt et al., 2012; Mungall et al., 2016).

616 The event at point E occurs where the aircraft was between cloud top and the top of the BL,
617 where no increases in UFP were observed before or after. It may be that the aircraft descended
618 slightly but sufficiently into the cloud-influenced area, which looks to be 25-40 m above cloud
619 top (Figure 9g), but also at that point we were in vicinity of Prince Leopold Island which is a bird
620 sanctuary and many bird colonies nest at the 260m high cliff. FLEXPART-WRF and the in-situ
621 wind measurement show that air masses to a large extent were directly coming off the island
622 (Figure 10, point E) suggesting a connection between the appearance of UFP and possible
623 emissions from the fauna of the island. The increase of particle phase ammonium (Figure 9d) at
624 the same time supports this connection and nucleation of particles from biogenic precursors
625 emitted by bird colonies are documented (Weber et al., 1998; Wentworth et al., 2016, Croft et al.
626 2016b).

627 Alternatively, it should be considered that evaporating fog and cloud droplets may also act as a
628 primary source of UFP (e.g. Heintzenberg et al., 2006; Karl et al., 2013; Leck and Bigg, 1999).
629 Karl et al., (2013) suggested a combined pathway that involves the emission of UFP by fog and
630 cloud droplets, together with secondary processes enabling growth of these particles. For our
631 observations we have no reason to assume that nucleation does not occur since conditions are
632 ideal but we cannot rule out that nanoparticles are emitted by the possibly evaporating cloud
633 droplets onto which gases then condense.

634 In conclusion the aerosol mass within the near surface layer is dominated by organics relative to
635 sulphate, while at just slightly higher altitude sulphate is clearly increased and increases further
636 above the inversion layer. A high organic content coincides with increases in UFP particles,
637 especially at times when also growth into the size range up to 50nm is indicated. Similarly the
638 MSA-to-sulphate ratio shows a peak at the lowest altitudes with maximum values in the vicinity
639 of clouds that coincide with a long residence time (~20h) of the air masses within the BL and
640 above open water. The data thereby suggest a marine biogenic influence of the aerosol within the
641 lower layers of the atmosphere. We note that similarly high levels of aerosol organics and MSA

were observed during the flight on July 12 associated with a NPF event and growth but in cloud-free conditions Willis et al. (2016).

4.4 CCN activity

CCN concentrations were measured at a supersaturation of 0.6%. The vertical profiles of CCN concentrations (Figure 11a) show patterns similar to those of larger particles. In the very clean boundary layer of the Arctic air mass period and the transition day CCN concentrations are equally low (~70 cm^{-3} and ~50 cm^{-3}, respectively). In contrast, southern air mass period average BL CCN concentrations are amongst the highest observed during this campaign (>300 cm^{-3}). Within the free troposphere CCN concentrations are surprisingly constant during the Arctic air mass period (120 ± 27 cm^{-3}) and more variable on the transition day (92 ± 46 cm^{-3}) and the southern air mass period (103 ± 67 cm^{-3}). The constant CCN concentrations during the Arctic air mass period correspond to the very uniform atmosphere dominated by aged aerosols we observed during this period and to the more layered atmosphere influenced by southern air masses possibly contaminated by biomass burning plumes during the later period. Correlations with $N_{>80}$ (Figure 11b) confirm that larger particles are a good approximation for these CCN concentrations. On average CCN concentrations agree to within ± 20 % of $N_{>80}$. However, it should be noted that slight differences between the 3 periods are indicated in the correlation curves: during the Arctic air mass period the average activation diameters are smaller than 80 nm, and during the southern air mass period they are larger than 80 nm. Assuming uniform chemical composition throughout the particle size range, an activation diameter of 80 nm at 0.6% supersaturation indicates an aerosol much less hygroscopic than, for example, ammonium sulphate; pure ammonium sulphate particles would activate at 40 m at 0.6% supersaturation. For the one specific event during which growth occurred (Willis et al., 2016), it was demonstrated that high CCN concentrations coincide with elevated organic mass loading. The reduced hygroscopicity of organic material relative to soluble inorganic salts (Petters and Kreidenweis, 2007) can explain the larger effective activation diameter.

A central question is whether and to what degree the CCN are influenced by the UFP. Two factors help with addressing this question: 1) particles as small as 20 nm and in general much

smaller than the average 80 nm size associated with the CCN at 0.6% will nucleate cloud droplets in the clean environment of the summer Arctic (Leaitch et al., 2016); 2) there is evidence here that increases in particles larger than 20 nm are associated with increases in the UFP, particularly for UFP influenced by cloud (e.g. Figure 8). Figure 12 shows regressions of CCN with UFP, $N_{>20}$, $N_{>30}$, $N_{>40}$ and $N_{>50}$. The high variability in the UFP and the time needed for a UFP particle to grow to an average size of 80 nm under these low precursor levels does not permit a direct connection of the CCN and UFP, but in all other cases, the main clusters of the regressions show quite similar and strong connections with the CCN measurements. Associations of the UFP with the $N_{>20}$ in the BL mean that some of these UFP are able to contribute to cloud-nucleating particles.

5 Discussion and Conclusions

This study presents airborne observations of ultrafine particles (UFP) during the Arctic summertime. Eleven flights were conducted in July 2014 in the area of Resolute Bay situated in the Canadian Archipelago. The location allowed access to open water, ice-covered regions and low clouds. Flights focused around the ice edge in Lancaster Sound including open waters to the east, the ice-covered region to the west, and polynas north of Resolute Bay. UFP were observed within all regions and above all terrains with the highest concentrations encountered in the boundary layer immediately above cloud and open water. It is shown that UFP occur most frequently (>65 % of the time) and with the highest concentrations (up to 5300 cm^{-3}) during an Arctic air mass period when the air is very clean and the boundary layer is thermally stable.

The frequent presence of UFP in the boundary layer over open water and low cloud and the enhanced number concentrations at the lowest altitudes sampled indicate a surface source, such as the ocean, for the UFP gaseous precursors. This is especially true during the Arctic air mass period when the sampling region was pristine and not influenced by pollution. FLEXPART-WRF simulations indicate that air masses had resided within the Arctic region at least 5-7 days prior to sampling. During this time UFP were restricted to the boundary layer and no UFP events were observed aloft, thereby excluding that these UFP form in the free troposphere and subside into the near surface layer e.g. (Clarke et al., 1998; Quinn and Bates, 2011). At the same time we

observed an extremely clean boundary layer (surface area of $N_{>40}$ ~5 $\mu m^2 m^{-3}$). Low surface areas increase the probability of particle formation via nucleation by reducing the surfaces for precursor gases to condense on.

Chlorophyll-a concentrations (Supplementary Figure 5) indicate a relatively high level of biological activity of the ocean (such as phytoplankton blooms known to produce DMS) throughout Lancaster Sound, to the east in Baffin Bay and in the open waters of the polynyas during the time period of the study. Indeed, measurements in Lancaster Sound performed from the Amundsen ice breaker just a few days after the aircraft campaign show that gas-phase DMS mixing ratios were high in the Lancaster Sound region (Mungall et al., 2016), up to 1155 ppt_v. DMS was also measured from the Polar 6 aircraft with an offline technique. Maximum mixing ratios of 110 ppt_v were detected in the surface layer (R. Ghahremaninezhad; personal communication), again confirming a marine influence in the boundary layer. The measured DMS concentrations are above the nucleation threshold obtained by modelling performed in the study of Chang et al. (2011) who concluded that DMS mixing ratios of $\geq$ 100ppt_v are sufficient to account for the formation of hundreds of UFP when background particle concentrations are low.

Relating observations of UFP to the surface below during the Arctic air mass period revealed that the highest UFP concentrations occurred above low-level cloud and open water with averages of 1040 cm^{-3} and 560 cm^{-3}, respectively. Above low-level cloud N_{20-40} showed increased concentrations. This simultaneous increase in concentrations suggests that UFP grow into the 40 nm size range, where they can nucleate cloud droplets.

Overall, the summertime Arctic is an active region in terms of new particle formation, occasionally accompanied by growth. The value of these altitude profiles across a wide spatial extent, performed for the first time in this campaign, is that they demonstrate that this activity is largely confined to the boundary layer, and that the dominant source of small particles to the boundary layer does not arise by mixing from aloft but most likely from marine sources. For future studies, the relative impact of such natural sources of UFP needs to be evaluated with respect to potential new sources, such as may arise with increasing shipping.

Acknowledgements

The authors would like to thank a large number of people for their contributions to this work. We thank Kenn Borek Air, in particular the pilots Kevin Elke and John Bayes and the aircraft engineer Kevin Riehl. We are grateful to John Ford, David Heath and the University of Toronto machine shop for safely mounting our instruments on racks for aircraft deployment. We thank Jim Hodgson and Lake Central Air Services in Muskoka, Jim Watson (Scale Modelbuilders, Inc.), Julia Binder and Martin Gerhmann (Alfred Wegener Institute, Helmholtz Center for Polar Marine Research, AWI), Mike Harwood and Andrew Elford (Environment and Climate Change Canada, ECCC), for their support of the integration of the instrumentation and aircraft. We gratefully acknowledge Carrie Taylor (ECCC), Bob Christensen (U of T), Lukas Kandora, Manuel Sellmann and Jens Herrmann (AWI), Desiree Toom, Sangeeta Sharma, Dan Veber, Andrew Platt, Anne Marie Macdonald, Ralf Staebler and Maurice Watt (ECCC) for their support of the study. We thank the Biogeochemistry department of MPIC for providing the CO instrument and Dieter Scharffe for his support during the preparation phase of the campaign. The authors J.L. Thomas and K.S. Law acknowledge funding support from the European Union under Grant Agreement n_ 5265863 – ACCESS (Arctic Climate Change, Economy and Society) project (2012-2015) and TOTAL SA. Computer simulations were performed on the IPSL mesoscale computer center (Mésocentre IPSL), which includes support for calculations and data storage facilities. We thank the Nunavut Research Institute and the Nunavut Impact Review Board for licensing the study. Logistical support in Resolute Bay was provided by the Polar Continental Shelf Project (PCSP) of Natural Resources Canada under PCSP Field Project #218614, and we are particularly grateful to Tim McCagherty and Jodi MacGregor of the PCSP. Funding for this work was provided by the Natural Sciences and Engineering Research Council of Canada through the NETCARE project of the Climate Change and Atmospheric Research Program, the Alfred Wegener Institute, Helmholtz Center for Polar and Marine Research and Environment and Climate Change Canada.

References

Aliabadi, A. A., Staebler, R. M., Liu, M. and Herber, A.: Characterization and Parametrization of Reynolds Stress and Turbulent Heat Flux in the Stably-Stratified Lower Arctic Troposphere Using Aircraft Measurements, Boundary-Layer Meteorol., doi:10.1007/s10546-016-0164-7, 2016a.

Aliabadi, A. A., Staebler, R. M., de Grandpré, J., Zadra, A. and Vaillancourt, P. A.: Comparison of Estimated Atmospheric Boundary Layer Mixing Height in the Arctic and Southern Great Plains under Statically Stable Conditions: Experimental and Numerical Aspects, Atmosphere-Ocean, 54(1), 60–74, doi:10.1080/07055900.2015.1119100, 2016b.

Asmi, E., Kondratyev, V., Brus, D., Laurila, T., Lihavainen, H., Backman, J., Vakkari, V., Aurela, M., Hatakka, J., Viisanen, Y., Uttal, T., Ivakhov, V. and Makshtas, A.: Aerosol size distribution seasonal characteristics measured in Tiksi, Russian Arctic, Atmos. Chem. Phys., 16(3), 1271–1287, doi:10.5194/acp-16-1271-2016, 2016.

Barrie, L. A.: Arctic air pollution: An overview of current knowledge, Atmos. Environ., 20(4), 643–663, doi:10.1016/0004-6981(86)90180-0, 1986.

Bigg, E. K. and Leck, C.: Properties of the aerosol over the central Arctic Ocean, J. Geophys. Res., 106(D23), 32101, doi:10.1029/1999JD901136, 2001.

Boé, J., Hall, A. and Qu, X.: September sea-ice cover in the Arctic Ocean projected to vanish by 2100, Nat. Geosci., 2(5), 341–343, doi:10.1038/ngeo467, 2009.

Brands, M., Kamphus, M., Böttger, T., Schneider, J., Drewnick, F., Roth, a., Curtius, J., Voigt, C., Borbon, a., Beekmann, M., Bourdon, a., Perrin, T. and Borrmann, S.: Characterization of a Newly Developed Aircraft-Based Laser Ablation Aerosol Mass Spectrometer (ALABAMA) and First Field Deployment in Urban Pollution Plumes over Paris During MEGAPOLI 2009, Aerosol Sci. Technol., 45(1), 46–64, doi:10.1080/02786826.2010.517813, 2011.

Brioude, J., Arnold, D., Stohl, A., Cassiani, M., Morton, D., Seibert, P., Angevine, W., Evan, S., Dingwell, A., Fast, J. D., Easter, R. C., Pisso, I., Burkhart, J. and Wotawa, G.: The Lagrangian particle dispersion model FLEXPART-WRF version 3.1, Geosci. Model Dev., 6(6), 1889–1904,

780 doi:10.5194/gmd-6-1889-2013, 2013.

781 Browse, J., Carslaw, K. S., Arnold, S. R., Pringle, K. and Boucher, O.: The scavenging processes
782 controlling the seasonal cycle in Arctic sulphate and black carbon aerosol, Atmos. Chem. Phys.,
783 12(15), 6775–6798, doi:10.5194/acp-12-6775-2012, 2012.

784 Browse, J., Carslaw, K. S., Mann, G. W., Birch, C. E., Arnold, S. R. and Leck, C.: The complex
785 response of Arctic aerosol to sea-ice retreat, Atmos. Chem. Phys., 14(14), 7543–7557,
786 doi:10.5194/acp-14-7543-2014, 2014.

787 Carslaw, K. S., Lee, L. A., Reddington, C. L., Pringle, K. J., Rap, A., Forster, P. M., Mann, G.
788 W., Spracklen, D. V, Woodhouse, M. T., Regayre, L. A. and Pierce, J. R.: Large contribution of
789 natural aerosols to uncertainty in indirect forcing., Nature, 503(7474), 67–71,
790 doi:10.1038/nature12674, 2013.

791 Chang, R. Y. W., Sjostedt, S. J., Pierce, J. R., Papakyriakou, T. N., Scarratt, M. G., Michaud, S.,
792 Levasseur, M., Leaitch, W. R. and Abbatt, J. P. D.: Relating atmospheric and oceanic DMS
793 levels to particle nucleation events in the Canadian Arctic, J. Geophys. Res. Atmos., 116(21), 1–
794 10, doi:10.1029/2011JD015926, 2011.

795 Charlson, R. J., Lovelock, J. E., Andreae, M. O. and Warren, S. G.: Oceanic phytoplankton,
796 atmospheric sulphur, cloud albedo and climate, Nature, 326, 655–661, doi:10.1038/326655a0,
797 1987.

798 Clarke, A. D., L, V. J., Eisele, F., Mauldin, R. L., Tanner, D. and M, L.: Particle production in
799 the remote marine atmosphere : Cloud outflow and subsidence during ACE 1, Earth Sci., 103,
800 1998.

801 Clarke, A. D., Kapustin, V. N., Eisele, F. L., Weber, R. J. , and McMurry, P. H.: Particle
802 production near marine clouds: sulfuric acid and predictions from classical binary nucleation,
803 Geophys. Res. Lett., 26, 2425-2428, doi: 10.1029/1999GL900438, 1999.

804 Covert, D. S., Wiedensohler, A., Aalto, P., Heintzenberg, J., McMurry, P. H. and Leck, C.:
805 Aerosol number size distributions from 3 to 500 nm diameter in the arctic marine boundary layer
806 during summer and autumn, Tellus, Ser. B Chem. Phys. Meteorol., 48(2), 197–212, 1996.

807 Croft, B., Martin, R. V., Leaitch, W. R., Tunved, P., Breider, T. J., D'Andrea, S. D. and Pierce, J.
808 R.: Processes controlling the seasonal cycle of Arctic aerosol number and size distributions,
809 Atmos. Chem. Phys., 16, 3665-3682, doi:10.5194/acp-16-3665-2016, 2016a.

810 Croft, B., G.R. Wentworth, R.V. Martin, W.R. Leaitch, J.G. Murphy, B.N. Murphy, J. Kodros,
811 J.P.D. Abbatt and J.R. Pierce. Contribution of Arctic seabird-colony ammonia to atmospheric
812 particles and cloud-albedo radiative effect. Nat. Commun. 7, 13444, doi: 10.1038/ncomms13444,
813 2016b.

814 DeCarlo, P. F., Kimmel, J. R., Trimborn, A., Northway, M. J., Jayne, J. T., Aiken, A. C., Gonin,
815 M., Fuhrer, K., Horvath, T., Docherty, K. S., Worsnop, D. R. and Jimenez, J. L.: Field-
816 deployable, high-resolution, time-of-flight aerosol mass spectrometer., Anal. Chem., 78(24),
817 8281–9, doi:10.1021/ac061249n, 2006.

818 Engvall, A.-C., Krecji, R., Sröm, J., Minikin, A., Treffeisen, R., Stohl, A. and Herber, A.: In-situ
819 airborne observations of the microphysical properties of the Arctic tropospheric aerosol during
820 late spring and summer, Tellus B, 0(0), 080414161623888–???, doi:10.1111/j.1600-
821 0889.2008.00348.x, 2008.

822 Engvall, a.-C., Krejci, R., Ström, J., Treffeisen, R., Scheele, R., Hermansen, O. and Paatero, J.:
823 Changes in aerosol properties during spring-summer period in the Arctic troposphere, Atmos.
824 Chem. Phys., 8, 445-462, doi:10.5194/acp-8-445-2008, 2008.

825 Garrett, T. J.: Effects of varying aerosol regimes on low-level Arctic stratus, Geophys. Res. Lett.,
826 31(17), L17105, doi:10.1029/2004GL019928, 2004.

827 Garrett, T. J., Hobbs, P. V and Radke, L. F.: High Aitken Nucleus Concentrations above Cloud
828 Tops in the Arctic, J. Atmos. Sci., 59(3), 779–783, doi:10.1175/1520-
829 0469(2001)059<0779:HANCAC>2.0.CO;2, 2002.

830 Garrett, T. J., Brattström, S., Sharma, S., Worthy, D. E. J. and Novelli, P.: The role of
831 scavenging in the seasonal transport of black carbon and sulfate to the Arctic, Geophys. Res.
832 Lett., 38(16), 1–6, doi:10.1029/2011GL048221, 2011.

833 Ge, X., Wexler, A. S. and Clegg, S. L.: Atmospheric amines - Part I. A review, Atmos. Environ.,
834 45(3), 524–546, doi:10.1016/j.atmosenv.2010.10.012, 2011.

835 Gibb, S. W., Mantoura, R. F. C. and Liss, P. S.: Ocean-atmosphere exchange and atmospheric
836 speciation of ammonia and methylamines in the region of the NW Arabian Sea, Global
837 Biogeochem. Cycles, 13(1), 161–178, doi:10.1029/98GB00743, 1999.

838 Hegg, D. A., Radke, L. F. and Hobbs, P. V: Particle production associated with marine clouds, J.
839 Geophys. Res. Atmos., 95(D9), 13917–13926, 1990.

840 Heintzenberg, B. J.: Particle size distribution and optical properties, Tellus, 32, 251–260,
841 10.1111/j.2153-3490.1980.tb00952.x, 1980.

842 Heintzenberg, B., Ström, J., Ogren, J. A., and Fimpel, H.-P.: Vertical profiles of aerosol
843 properties in the summer troposphere of central Europe, scandinavia and the svalbard region,
844 Atmos. Env., 25, 621-627, doi: 10.1016/0960-1686(91)90059-G, 1991.

845 Heintzenberg, B., and Leck, C.: Seasonal variation of the atmospheric aerosol near the top of the
846 marine boundary layer over Spitsbergen related to the Arctic sulphur cycle. Tellus B, 46, 52-67,
847 doi: 10.1034/j.1600-0889.1994.00005.x, 1994.

848 Heintzenberg, J., Leck, C., Birmili, W., Wehner, B., Tjernström, M., Wiedensohler, A.,
849 Tjernstrom, M. and Wiedensohler, A.: Aerosol number-size distributions during clear and fog
850 periods in the summer high Arctic: 1991, 1996 and 2001, Tellus B, 58(1), 41–50,
851 doi:10.1111/j.1600-0889.2005.00171.x, 2006.

852 Heintzenberg, J. and Leck, C.: The summer aerosol in the central Arctic 1991–2008: did it
853 change or not?, Atmos. Chem. Phys., 12(9), 3969–3983, doi:10.5194/acp-12-3969-2012, 2012.

854 Heintzenberg, J., Leck, C. and Tunved, P.: Potential source regions and processes of aerosol in
855 the summer Arctic, Atmos. Chem. Phys., 15(11), 6487–6502, doi:10.5194/acp-15-6487-2015,
856 2015.

857 Hoppel, W. a., Frick, G. M., Fitzgerald, J. W. and Larson, R. E.: Marine boundary layer
858 measurements of new particle formation and the effects nonprecipitating clouds have on aerosol
859 size distribution, J. Geophys. Res., 99(D7), 14443, doi:10.1029/94JD00797, 1994.

860 Karl, M., Leck, C., Gross, A. and Pirjola, L.: A study of new particle formation in the marine
861 boundary layer over the central Arctic Ocean using a flexible multicomponent aerosol dynamic

862 model, Tellus B, 64(0), 1–24, doi:10.3402/tellusb.v64i0.17158, 2012.

863 Karl, M., Leck, C., Coz, E. and Heintzenberg, J.: Marine nanogels as a source of atmospheric
864 nanoparticles in the high Arctic, Geophys. Res. Lett., 40(14), 3738–3743, doi:10.1002/grl.50661,
865 2013.

866 Kulmala, M., Dal Maso, M., Mäkelä, J. M., Pirjola, L., Väkevä, M., Aalto, P., Miikkulainen, P.,
867 Hämeri, K. and O'Dowd, C. D.: On the formation, growth and composition of nucleation mode
868 particles, Tellus, Ser. B Chem. Phys. Meteorol., 53, 479–490, doi:10.1034/j.1600-
869 0889.2001.d01-33.x, 2001.

870 Kupiszewski, P., Leck, C., Tjernström, M., Sjogren, S., Sedlar, J., Graus, M., M??ller, M.,
871 Brooks, B., Swietlicki, E., Norris, S. and Hansel, A.: Vertical profiling of aerosol particles and
872 trace gases over the central Arctic Ocean during summer, Atmos. Chem. Phys., 13(24), 12405–
873 12431, doi:10.5194/acp-13-12405-2013, 2013.

874 Law, K. S., Stohl, A., Quinn, P. K., Brock, C. A., Burkhart, J. F., Paris, J. D., Ancellet, G.,
875 Singh, H. B., Roiger, A., Schlager, H., Dibb, J., Jacob, D. J., Arnold, S. R., Pelon, J. and
876 Thomas, J. L.: Arctic air pollution: New insights from POLARCAT-IPY, Bull. Am. Meteorol.
877 Soc., 95(12), 1873–1895, doi:10.1175/BAMS-D-13-00017.1, 2014.

878 Leaitch, W.R., Hoff, R.M., Melnichuk, S., and Hogan, W.: Some chemical and physical
879 properties of the Arctic winter aerosol in northeastern Canada. J. Climate Appl. Meteorol., 23,
880 916-928, http://dx.doi.org/10.1175/1520-0450(1984)023<0916:SPACPO>2.0.CO;2, 1984.

881 Leaitch, W.R., Barrie, L.A., Bottenheim, J.W., Li, S.-M., Shepson, P. and Yokouchi, Y.:
882 Airborne observations related ozone depletion at polar sunrise. J. Geophys. Res., 99, 25499-
883 25517, 10.1029/94JD02750, 1994.

884 Leaitch, W. R., Sharma, S., Huang, L., Toom-Sauntry, D., Chivulescu, A., Macdonald, A. M.,
885 von Salzen, K., Pierce, J. R., Bertram, A. K., Schroder, J. C., Shantz, N. C., Chang, R. Y. W. and
886 Norman, A.-L.: Dimethyl sulfide control of the clean summertime Arctic aerosol and cloud,
887 Elem. Sci. Anth., 1(1), 17, doi:10.12952/journal.elementa.000017, 2013.

888 Leaitch, W. R., Korolev, A., Aliabadi, A. A., Burkart, J., Willis, M., Abbatt, J. P. D., Bozem, H.,
889 Hoor, P., Köllner, F., Schneider, J., Herber, A., Konrad, C. and Brauner, R.: Effects of 20-100

890 nanometre particles on liquid clouds in the clean summertime Arctic, Atmos. Chem. Phys., 16,
891 11107-11124, doi:10.5194/acp-16-11107-2016, 2016.

892 Leck, C. and Bigg, E. K.: Aerosol production over remote marine areas-A new route, Geophys.
893 Res. Lett., 26(23), 3577, doi:10.1029/1999GL010807, 1999.

894 Leck, C. and Bigg, E. K.: Source and evolution of the marine aerosol - A new perspective,
895 Geophys. Res. Lett., 32(19), 1–4, doi:10.1029/2005GL023651, 2005.

896 Leck, C. and Bigg, E. K.: New Particle Formation of Marine Biological Origin, Aerosol Sci.
897 Technol., 44(7), 570–577, doi:10.1080/02786826.2010.481222, 2010.

898 Lohmann, U. and Feichter, J.: Global indirect aerosol effects: a review, Atmos. Chem. Phys., 5,
899 715–735, doi:10.5194/acp-5-715-2005, 2005.

900 Mauldin, R. L., Madronich, S., Flocke, S. J. , Eisele, F. L. , Frost, G. J. and Prevot, A. S. H. :
901 New insights on OH: Measurements around and in clouds, Geophys. Res. Lett., 24(No 23),
902 3033-3036, doi:10.1029/97GL02983, 1997.

903 Mauritsen, T., Sedlar, J., Tjernström, M., Leck, C., Martin, M., Shupe, M., Sjogren, S., Sierau,
904 B., Persson, P. O. G., Brooks, I. M. and Swietlicki, E.: An Arctic CCN-limited cloud-aerosol
905 regime, Atmos. Chem. Phys., 11(1), 165–173, doi:10.5194/acp-11-165-2011, 2011.

906 Mungall, E. L., Croft, B., Lizotte, M., Thomas, J. L., Murphy, J. G., Levasseur, M., Martin, R.
907 V., Wentzell, J. J. B., Liggio, J. and Abbatt, J. P. D.: Dimethyl sulfide in the summertime Arctic
908 atmosphere: measurements and source sensitivity simulations, Atmos. Chem. Phys., 16(11),
909 6665–6680, doi:10.5194/acp-16-6665-2016, 2016.

910 Nguyen, Q. T., Glasius, M., Sørensen, L. L., Jensen, B., Skov, H., Birmili, W., Wiedensohler, A.,
911 Kristensson, A., Nøjgaard, J. K. and Massling, A.: Seasonal variation of atmospheric particle
912 number concentrations, new particle formation and atmospheric oxidation capacity at the high
913 Arctic site Villum Research Station, Station Nord, Atmos. Chem. Phys. Discuss., 1–41,
914 doi:10.5194/acp-2016-205, 2016.

915 Petters, M. D. and Kreidenweis, S. M.: A single parameter representation of hygroscopic growth
916 and cloud condensation nucleus activity, Atmos. Chem. Phys., 7, 1961–1971, 2007.

917 Pierce, J. R., Leaitch, W. R., Liggio, J., Westervelt, D. M., Wainwright, C. D., Abbatt, J. P. D.,
918 Ahlm, L., Al-Basheer, W., Cziczo, D. J., Hayden, K. L., Lee, A. K. Y., Li, S.-M., Russell, L. M.,
919 Sjostedt, S. J., Strawbridge, K. B., Travis, M., Vlasenko, A., Wentzell, J. J. B., Wiebe, H. A.,
920 Wong, J. P. S., and Macdonald, A. M.: Nucleation and condensational growth to CCN sizes
921 during a sustained pristine biogenic SOA event in a forested mountain valley, Atmos. Chem.
922 Phys., 12, 3147-3163, doi:10.5194/acp-12-3147-2012, 2012.

923 Pirjola, L., O'Dowd, C. D., Brooks, I. M. and Kulmala, M.: Can new particle formation occur in
924 the clean marine boundary layer?, J. Geophys. Res. Atmos., 105(D21), 26531–26546,
925 doi:10.1029/2000JD900310, 2000.

926 Quinn, P. K. and Bates, T. S.: The case against climate regulation via oceanic phytoplankton
927 sulphur emissions, Nature, 480(7375), 51–56, doi:10.1038/nature10580, 2011.

928 Quinn, P. K., Shaw, G., Andrews, E., Dutton, E. G., Ruoho-Airola, T. and Gong, S. L.: Arctic
929 haze: Current trends and knowledge gaps, Tellus, Ser. B Chem. Phys. Meteorol., 59(1), 99–114,
930 doi:10.1111/j.1600-0889.2006.00238.x, 2007.

931 Radke, F. L. and Hobbs, P. V.: Humidity and particle fields around some small cumulus clouds,
932 Journal of atmospheric sciences, 48(9), 1190-1193, doi: http://dx.doi.org/10.1175/1520-
933 0469(1991)048<1190:HAPFAS>2.0.CO;2, 1991.

934 Rahn, K. A., Borys, R. D. and Shaw, G. E.: The Asian source of Arctic haze bands, Nature, 268,
935 713-715, doi: 10.1038/268713a0, 1977.

936 Rehbein, P. J. G., Jeong, C. H., McGuire, M. L., Yao, X., Corbin, J. C. and Evans, G. J.: Cloud
937 and fog processing enhanced gas-to-particle partitioning of trimethylamine, Environ. Sci.
938 Technol., 45(10), 4346–4352, doi:10.1021/es1042113, 2011.

939 Riipinen, I., Pierce, J. R., Yli-Juuti, T., Nieminen, T., Häkkinen, S., Ehn, M., Junninen, H.,
940 Lehtipalo, K., Petäjä, T., Slowik, J., Chang, R., Shantz, N. C., Abbatt, J., Leaitch, W. R.,
941 Kerminen, V.-M., Worsnop, D. R., Pandis, S. N., Donahue, N. M., and Kulmala, M.: Organic
942 condensation: a vital link connecting aerosol formation to cloud condensation nuclei (CCN)
943 concentrations, Atmos. Chem. Phys., 11, 3865-3878, doi:10.5194/acp-11-3865-2011, 2011.

Seinfeld, J.H., and Pandis, S. N.: Atmospheric Chemistry and Physics: From Air Pollution to Climate Change. 3rd Edition. John Wiley & Sons, Inc., 2016.

Shaw, G.E. and Stamnes, K.: Arctic haze: perturbations of the polar radiation budget. Ann. N. E Ad. Aci. 338, 533-539, doi: 10.1111/j.1749-6632.1980.tb17145.x 1980.

Shaw, G. E.: The Arctic Haze Phenomenon, Bull. Am. Meteorol. Soc., 76, 2403–2413, doi:10.1175/1520-0477(1995)076<2403:TAHP>2.0.CO;2, 1995.

Skamarock, W. C., Klemp, J. B., Dudhia, J., Gill, D. O., Barker, D. M., Wang, W. and Powers, J. G.: A Description of the Advanced Research WRF Version 2, [online] Available from: http://oai.dtic.mil/oai/oai?verb=getRecord&metadataPrefix=html&identifier=ADA487419 (Accessed 22 March 2016), 2005.

Sjostedt, S. J., Leaitch, W. R., Levasseur, M., Scarratt, M., Michaud, S., Motard-Côté, J., Burkhart, J. H., and Abbatt J.: Evidence for the uptake of atmospheric acetone and methanol by the Arctic Ocean during late summer DMS-Emission plumes. J. Geophys. Res., 117, D12303, doi: 10.1029/2011JD017086, 2012.

Stohl, a., Forster, C., Frank, A., Seibert, P. and Wotawa, G.: Technical note: The Lagrangian particle dispersion model FLEXPART version 6.2, Atmos. Chem. Phys. Discuss., 5(4), 4739–4799, doi:10.5194/acpd-5-4739-2005, 2005.

Ström, J., Umegård, J., Tørseth, K., Tunved, P., Hansson, H. C., Holmén, K., Wismann, V., Herber, A. and König-Langlo, G.: One year of particle size distribution and aerosol chemical composition measurements at the Zeppelin Station, Svalbard, March 2000-March 2001, Phys. Chem. Earth, 28(March 2000), 1181–1190, doi:10.1016/j.pce.2003.08.058, 2003.

Ström, J., Engvall, A. C., Delbart, F., Krejci, R. and Treffeisen, R.: On small particles in the Arctic summer boundary layer: Observations at two different heights near Ny-Ålesund, Svalbard, Tellus, Ser. B Chem. Phys. Meteorol., 61 B(2), 473–482, doi:10.1111/j.1600-0889.2008.00412.x, 2009.

Tjernström, M., Birch, C. E., Brooks, I. M., Shupe, M. D., Persson, P. O. G., Sedlar, J.,

971 Mauritsen, T., Leck, C., Paatero, J., Szczodrak, M. and Wheeler, C. R.: Meteorological
972 conditions in the central Arctic summer during the Arctic Summer Cloud Ocean Study
973 (ASCOS), Atmos. Chem. Phys., 12(15), 6863–6889, doi:10.5194/acp-12-6863-2012, 2012.

974 Tjernström, M., Leck, C., Birch, C. E., Bottenheim, J. W., Brooks, B. J., Brooks, I. M., Bäcklin,
975 L., Chang, R. Y. W., De Leeuw, G., Di Liberto, L., De La Rosa, S., Granath, E., Graus, M.,
976 Hansel, a., Heintzenberg, J., Held, a., Hind, a., Johnston, P., Knulst, J., Martin, M., Matrai, P.
977 a., Mauritsen, T., Müller, M., Norris, S. J., Orellana, M. V., Orsini, D. a., Paatero, J., Persson, P.
978 O. G., Gao, Q., Rauschenberg, C., Ristovski, Z., Sedlar, J., Shupe, M. D., Sierau, B., Sirevaag,
979 a., Sjogren, S., Stetzer, O., Swietlicki, E., Szczodrak, M., Vaattovaara, P., Wahlberg, N.,
980 Westberg, M. and Wheeler, C. R.: The Arctic Summer Cloud Ocean Study (ASCOS): Overview
981 and experimental design, Atmos. Chem. Phys., 14(6), 2823–2869, doi:10.5194/acp-14-2823-
982 2014, 2014.

983 Tunved, P., Ström, J. and Krejci, R.: Arctic aerosol life cycle: linking aerosol size distributions
984 observed between 2000 and 2010 with air mass transport and precipitation at Zeppelin station,
985 Ny-Ålesund, Svalbard, Atmos. Chem. Phys., 13(7), 3643–3660, doi:10.5194/acp-13-3643-2013,
986 2013.

987 Twomey, S.: Pollution and the Planetary Albedo, Atmos. Environ., 41(Vol. 8), 1251–1256,
988 doi:10.1016/j.atmosenv.2007.10.062, 1974.

989 Wang, M. and Overland, J. E.: A sea ice free summer Arctic within 30 years: An update from
990 CMIP5 models, Geophys. Res. Lett., 39(17), 2–6, doi:10.1029/2012GL052868, 2012.

991 Weber, R. J., McMurry, P. H., Mauldin, L., Tanner, D. J., Eisele, F. L., Brechtel, F. J.,
992 Kreidenweis, S. M., Kok, G. L., Schillawski, R. D. and Baumgardner, D.: A study of new
993 particle formation and growth involving biogenic and trace gas species measured during ACE 1,
994 J. Geophys. Res., 103(D13), 16385–16396, doi:10.1029/97JD02465, 1998.

995 Wentworth, G. R., Murphy, J. G., Croft, B., Martin, R. V., Pierce, J. R., Côté, J.-S., Courchesne,
996 I., Tremblay, J.-É., Gagnon, J., Thomas, J. L., Sharma, S., Toom-Sauntry, D., Chivulescu, a.,
997 Levasseur, M. and Abbatt, J. P. D.: Ammonia in the summertime Arctic marine boundary layer:
998 sources, sinks and implications, Atmos. Chem. Phys., 16, 1937-1953, doi:10.5194/acp-16-1937-

2016, 2016.

Wiedensohler, A., Covert, D. S., Swietlicki, E., Aalto, P., Heintzenberg, J. and Leck, C.: Occurrence of an ultrafine particle mode less than 20 nm in diameter in the marine boundary layer during Arctic summer and autumn, Tellus, Ser. B Chem. Phys. Meteorol., 48(2), 213–222, doi:10.1034/j.1600-0889.1996.t01-1-00006.x, 1996.

Wiedensohler, A. H.-C. Hansson, D. Orsini, M. Wendisch, F. Wagner, K.N. Bower, T.W. Chourlarton, M. Wells, M. Parkin, K. Acker, W. Wieprecht, M.C. Facchini, J.A. Lind, S. Fuzzi, B.G. Arends, M. Kulmalao: Night-time formation and occurrence of new particles associated with orographic clouds, Atmos. Env., 31(16), 2445-2559, doi: http://dx.doi.org/10.1016/S1352-2310(96)00299-3, 1997.

Willis, M. D., Burkart, J., Thomas, J. L., Köllner, F., Schneider, J., Bozem, H., Hoor, P. M., Aliabadi, A. A., Schulz, H., Herber, A. B., Leaitch, W. R. and Abbatt, J. P. D.: Growth of nucleation mode particles in the summertime Arctic: a case study, Atmos. Chem. Phys., 7663–7679, doi:10.5194/acp-16-7663-2016, 2016.

Zhang, J., Spitz, Y. H., Steele, M., Ashjian, C., Campbell, R., Berline, L. and Matrai, P.: Modeling the impact of declining sea ice on the Arctic marine planktonic ecosystem, J. Geophys. Res. Ocean., 115(10), 1–24, doi:10.1029/2009JC005387, 2010.

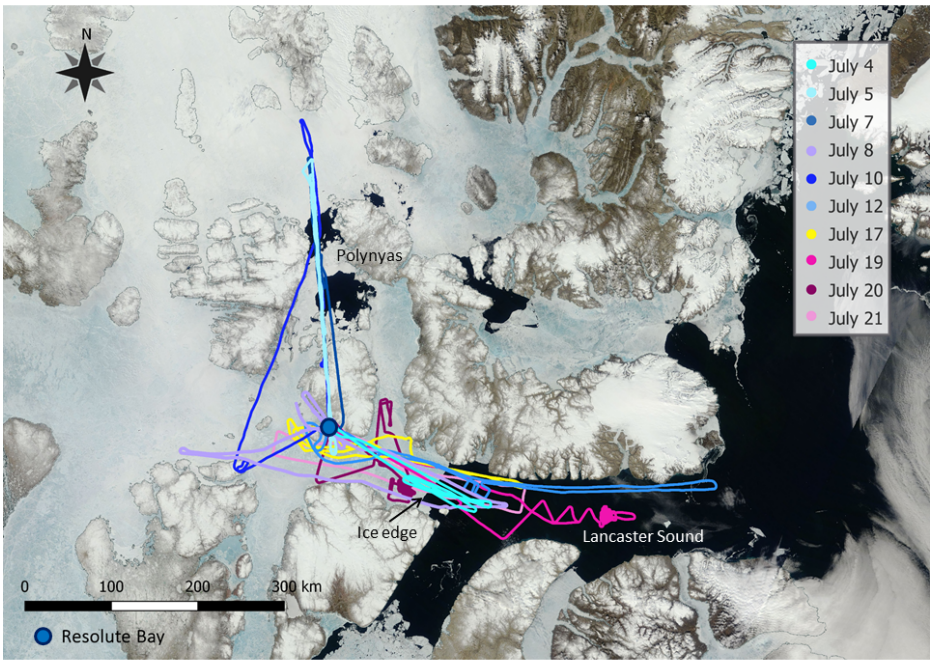

Figure 1. Compilation of all flight tracks plotted on a satellite image from July 4, 2014. The image is taken from: https://earthdata.nasa.gov/labs/worldview.

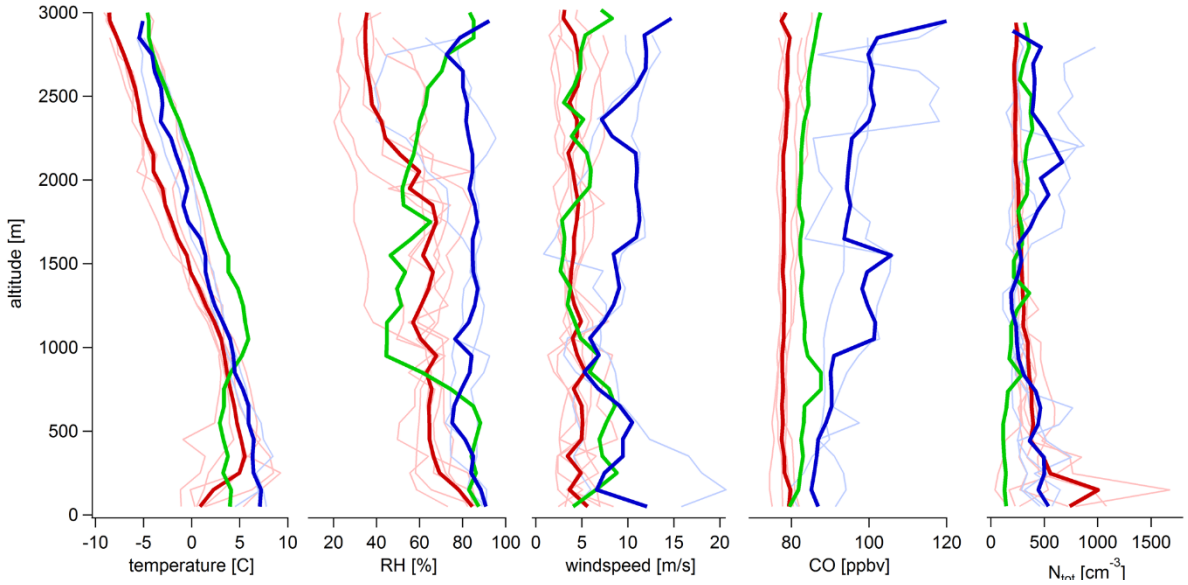

Figure 2. Median temperature, relative humidity (RH), wind speed,CO mixing ratio and N_{tot} profiles for the Arctic air mass period (dark red), the transition day (dark green), and the southern air mass period (dark blue). Median profiles for each flight are plotted in the background in the corresponding light colours.

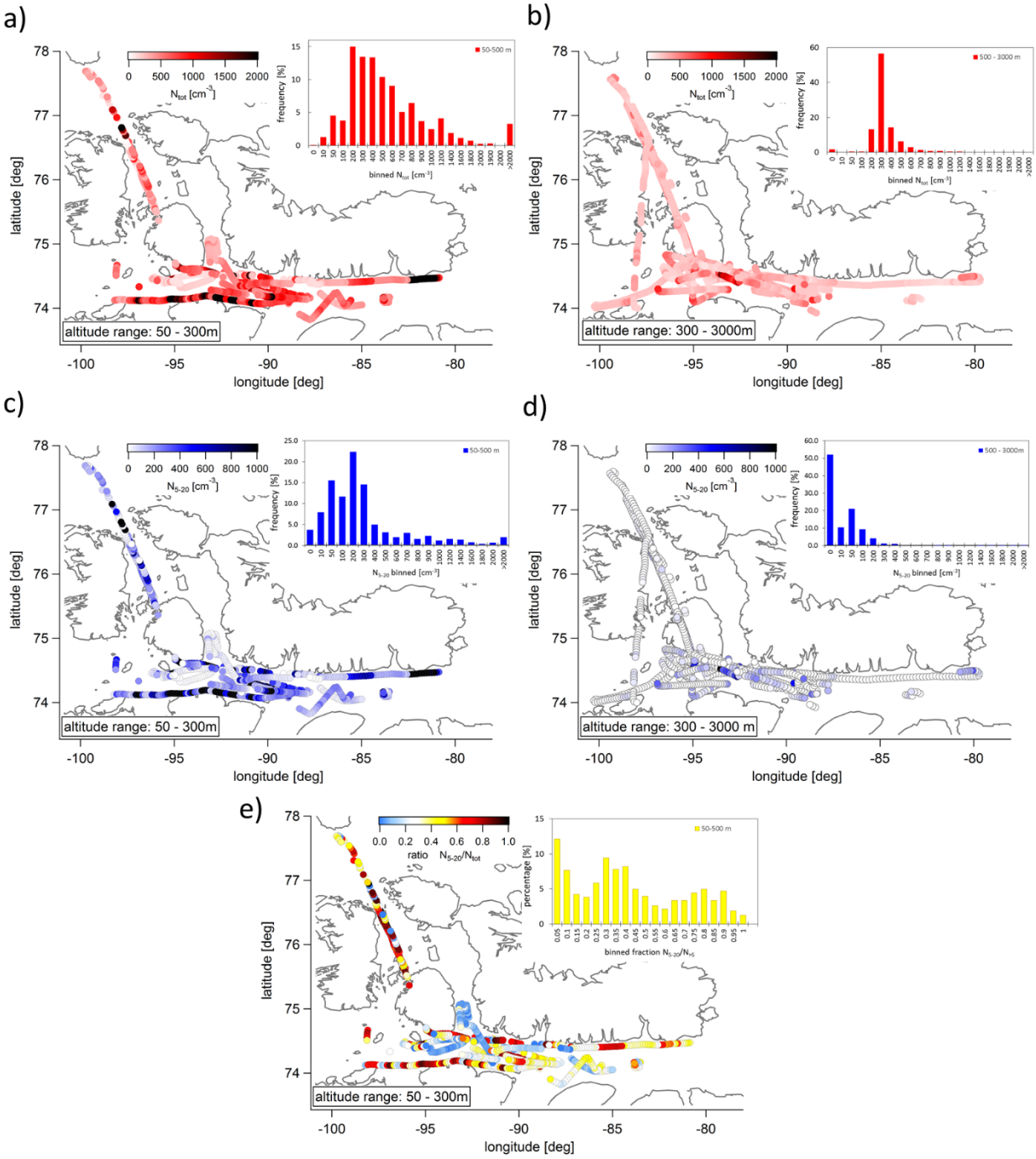

Figure 3. Flight tracks colour coded by particle concentrations. a.) Flight tracks within the boundary layer (50-300 m) colour coded by N_{tot}. b) Flight tracks within the free troposphere (300-3000 m) colour coded by N_{tot}. c) Flight tracks within the boundary layer (50-300m) colour

coded by UFP. d) Flight tracks within the free troposphere (300-3000 m) colour coded by $N_{5\text{-}20}$. e) Flight tracks within the boundary layer (50-300 m) colour coded by the ratio of $N_{5\text{-}20}/N_{tot}$

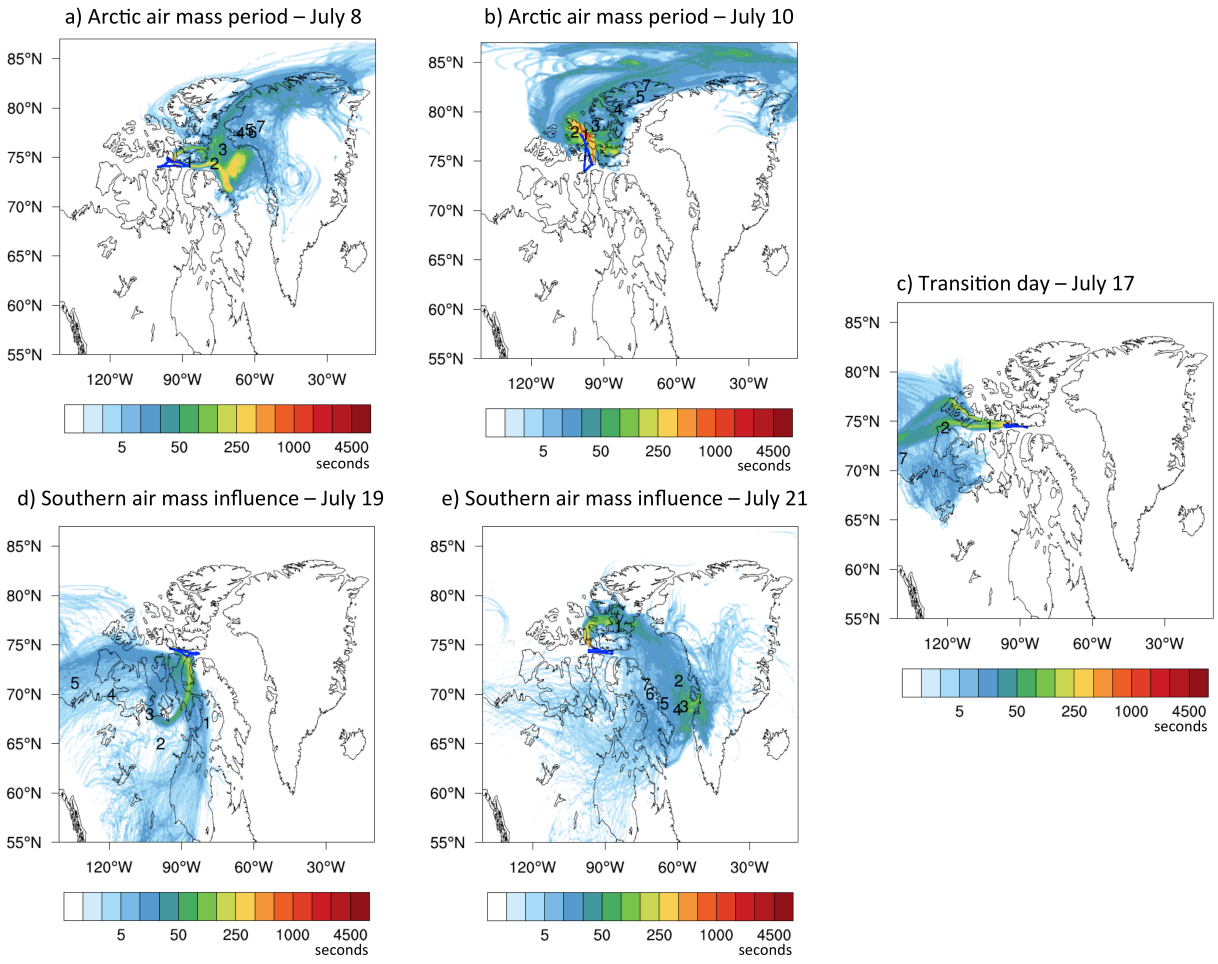

Figure 4. FLEXPART-WRF potential emissions sensitivities for each flight (using particle releases every 2 minutes along the flight track) that illustrate transport regimes during different periods of the campaign. The colour code indicates the residence time of air in seconds and the numbers represent the position of the plume centroid location in days prior to release (days 1-7).

Revised figure

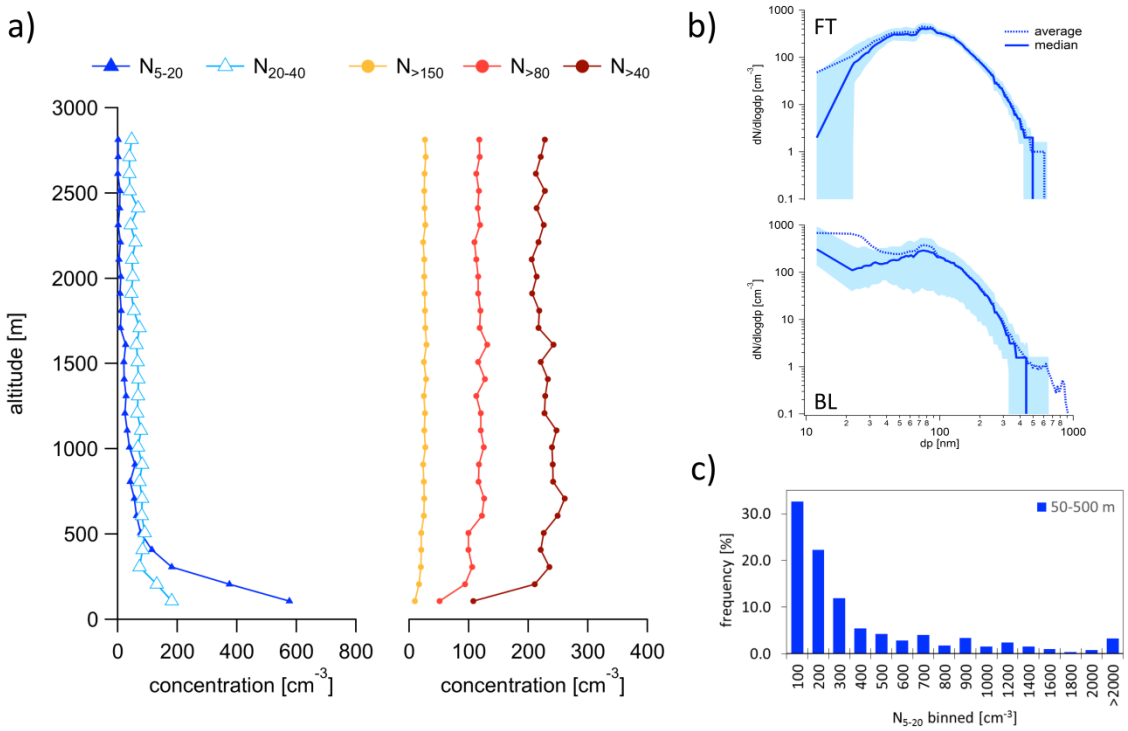

Figure 5. Average particle concentration data during the Arctic air mass period. a) Average vertical profiles of $N_{5\text{-}20}$, $N_{20\text{-}40}$, $N_{>40}$, $N_{>80}$, and $N_{>150}$. b) Average (solid line) and median (dashed line) size distribution within the BL and the FT. The light blue area represents the 25-75th % percentile range. c) Frequency distribution of the occurrence of UFP illustrates the large variability of the UFP concentrations within the BL.

Revised figure

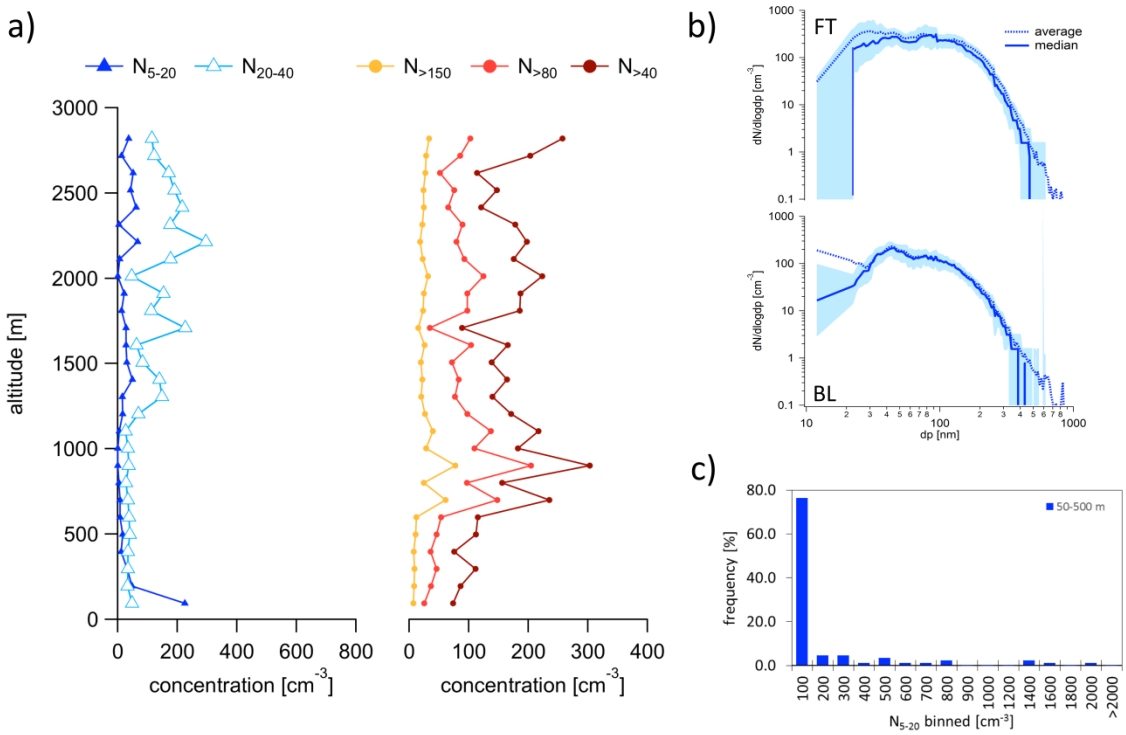

Figure 6. Average particle concentration data on the transition day. a) Average vertical profiles of $N_{5\text{-}20}$, $N_{20\text{-}40}$, $N_{>40}$, $N_{>80}$, and $N_{>150}$. b) Average (solid line) and median (dashed line) size distribution within the BL and the FT. The light blue area represents the 25-75th % percentile range. c) Frequency distribution of the occurrence of UFP illustrates the large variability of the UFP concentrations within the BL.

Revised figure

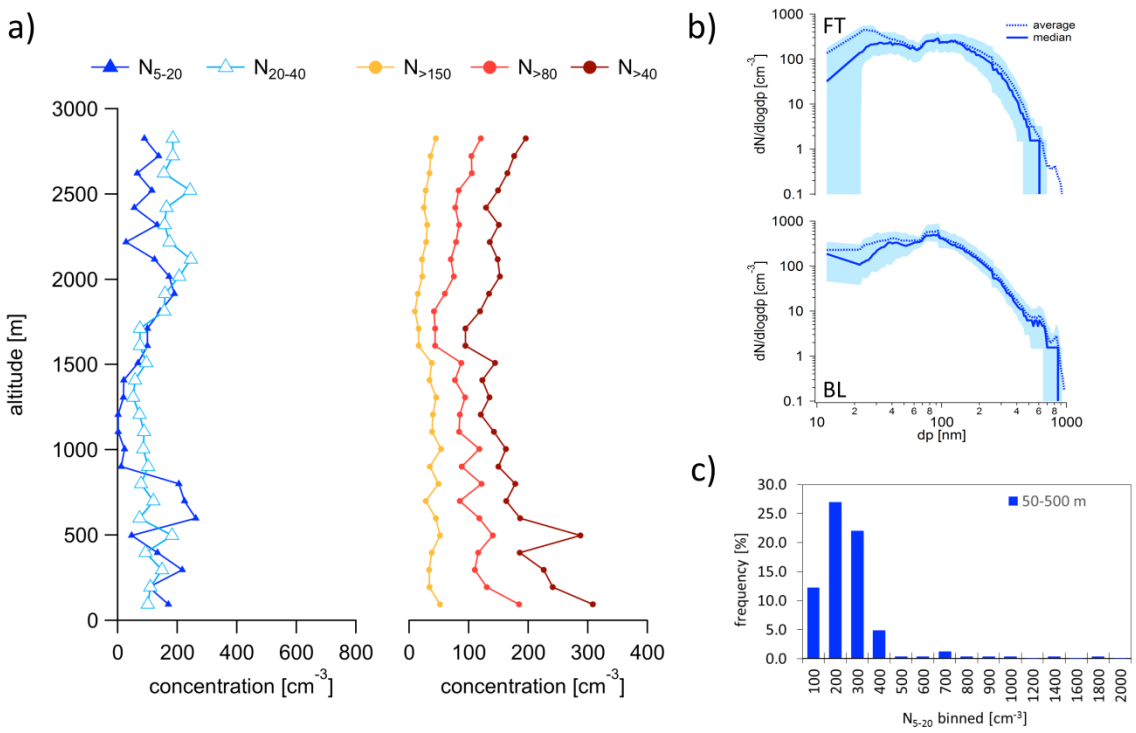

Figure 7. Average particle concentration data during the southern air mass period. a) Average vertical profiles of $N_{5\text{-}20}$, $N_{20\text{-}40}$, $N_{>40}$, $N_{>80}$, and $N_{>150}$. b) Average (solid line) and median (dashed line) size distribution within the BL and the FT. The light blue area represents the 25-75th % percentile range. c) Frequency distribution of the occurrence of UFP illustrates the large variability of the UFP concentrations within the BL.

Revised figure

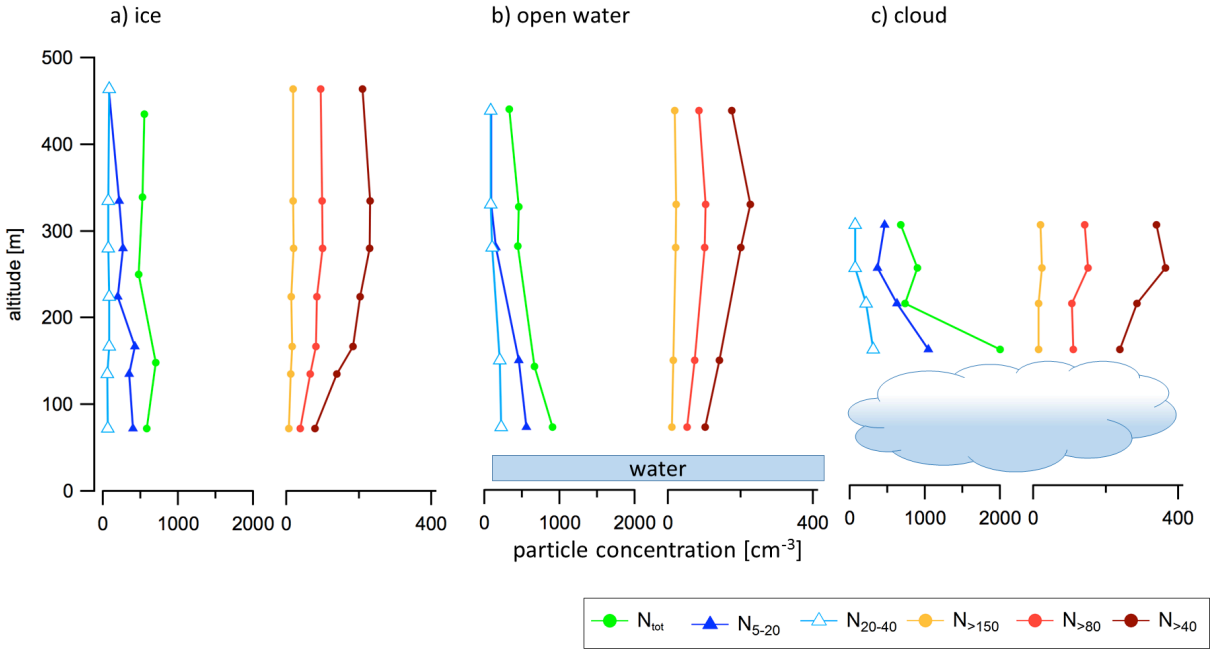

Figure 8. Average profiles of particle concentrations above ice, open water and cloud. The number of data points for each specific profile is: 130 above water, 216 above cloud, and 123 above water.

1072 revised figure

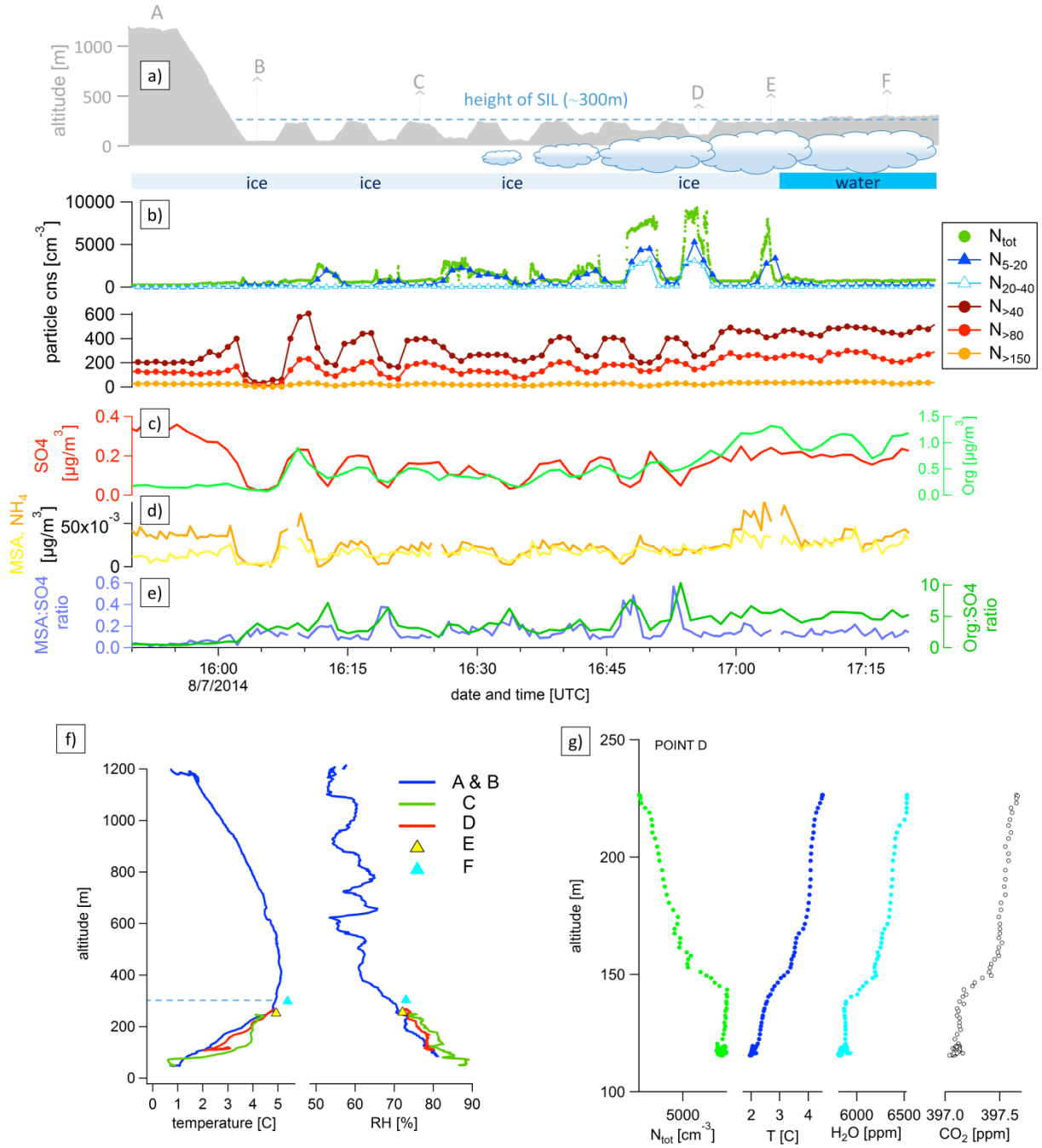

1073

1074 Figure 9. Case study from July 8 flight. Time series of flight altitude and illustration of the
1075 surface including cloud coverage (a), aerosol size (b) and chemical composition (c-e). (f)

1076 Vertical profiles of temperature and RH at locations A-F. (g) N_{tot}, temperature, H_2O mixing ratio
1077 and CO_2 profiles at location D.

1078

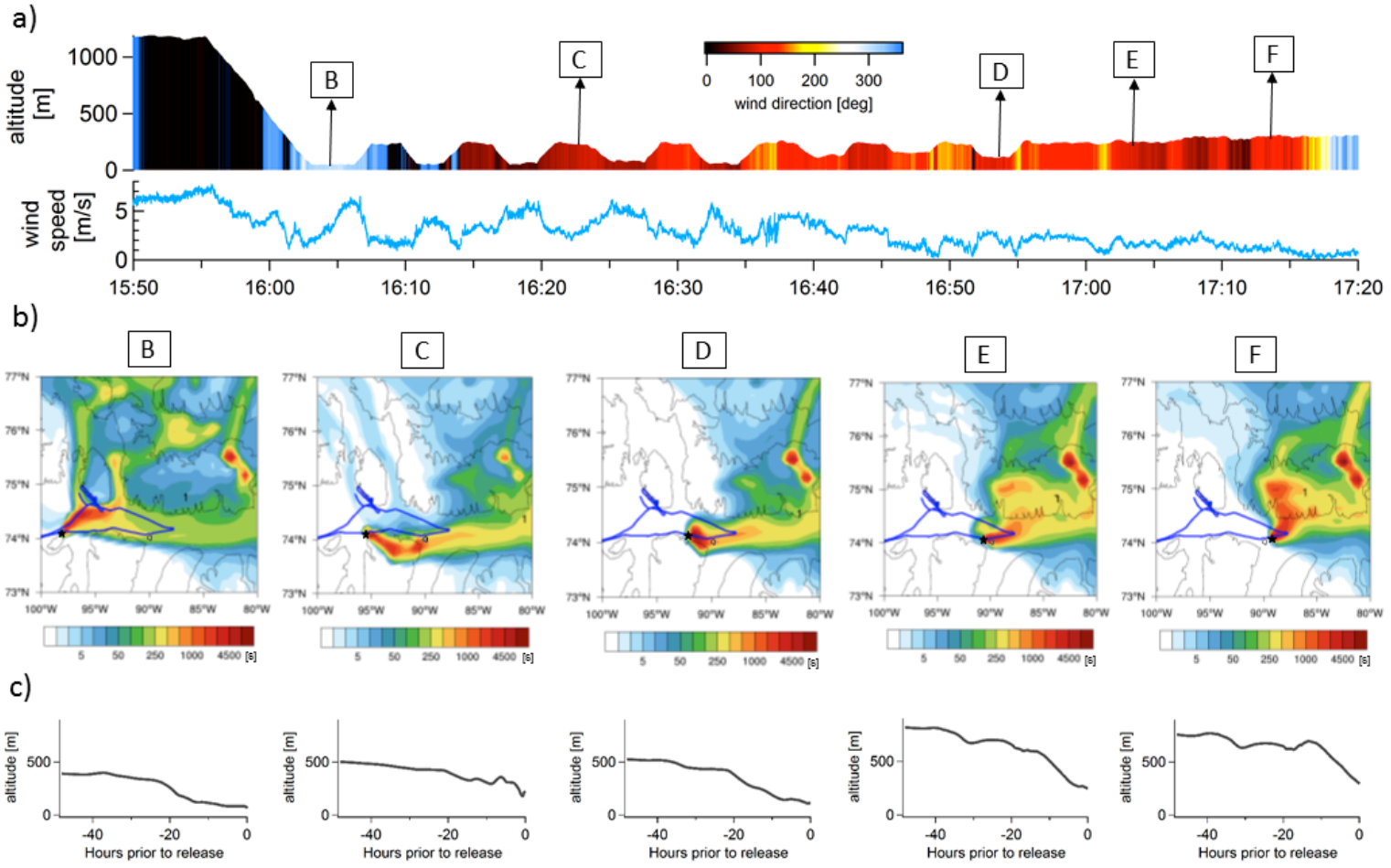

1079

1080

Figure 10. (a) Time series of aircraft altitude color coded with the wind direction and time series of wind speed (b) FLEXPART-WRF seven day backwards potential emissions sensitivities for points along the flight track (60 second release at time at indicated time and location) showing the air mass history at 5 representative locations within the SIL. The plume centroid location for particles with age of one day is indicated. (c) The bottom plots show the altitude of plume centroid 48 hours back in time.

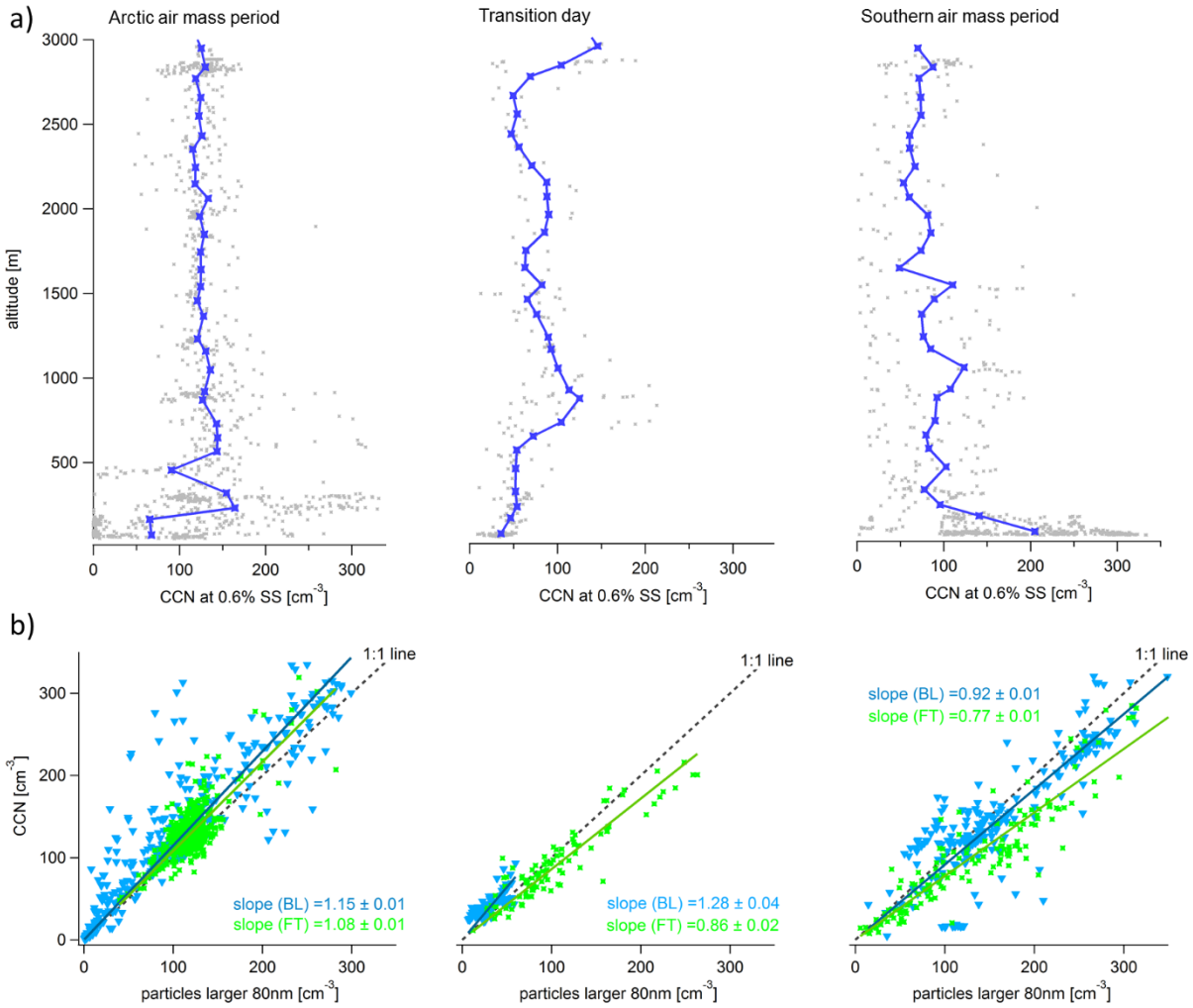

Figure 11. (a) Vertical profiles of average CCN concentrations (dark blue). All data points are plotted in light grey. (b) Correlation plots between CCN concentrations and particles larger than 80nm.

added figure

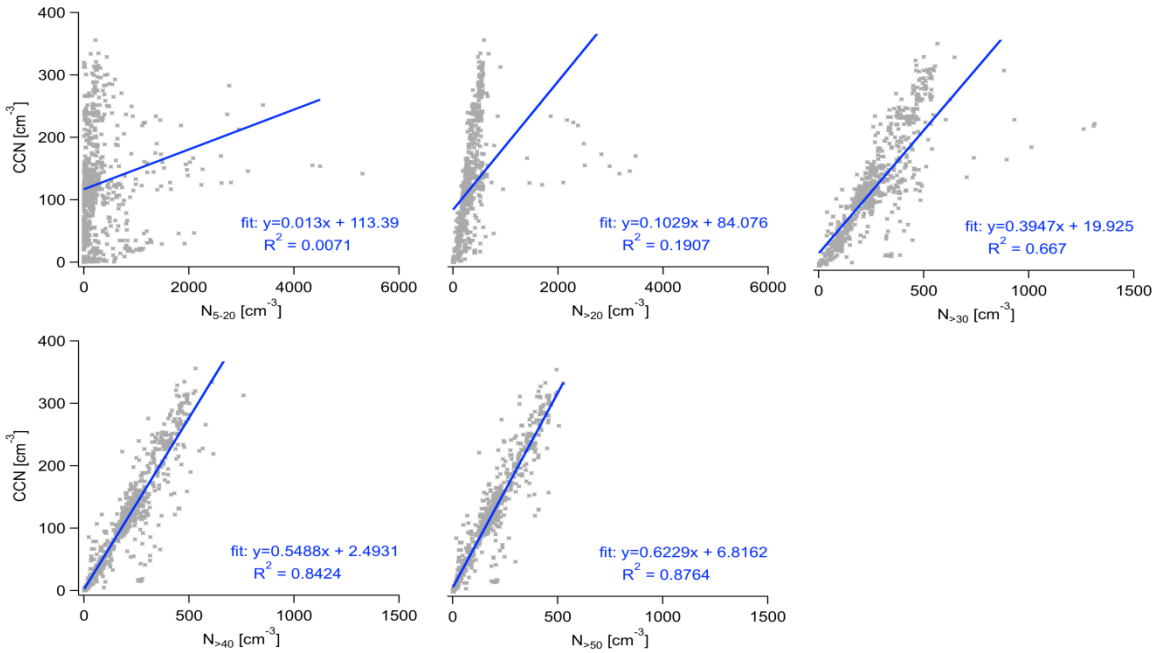

Figure 12. Correlations between CCN and particle concentrations for the full study period.

Supplemental Material

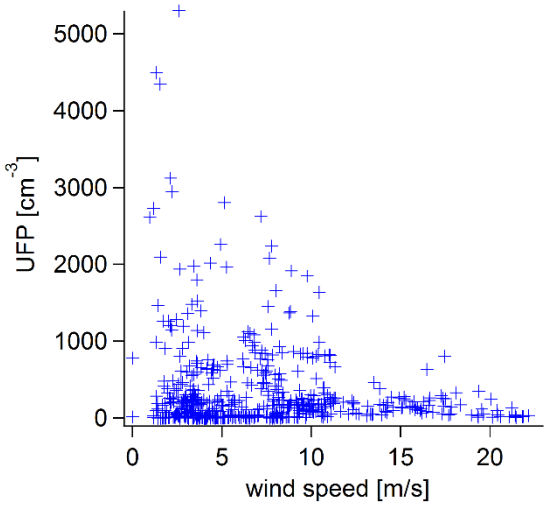

S Figure 1. UFP vs wind speed within the BL for the entire campaign.

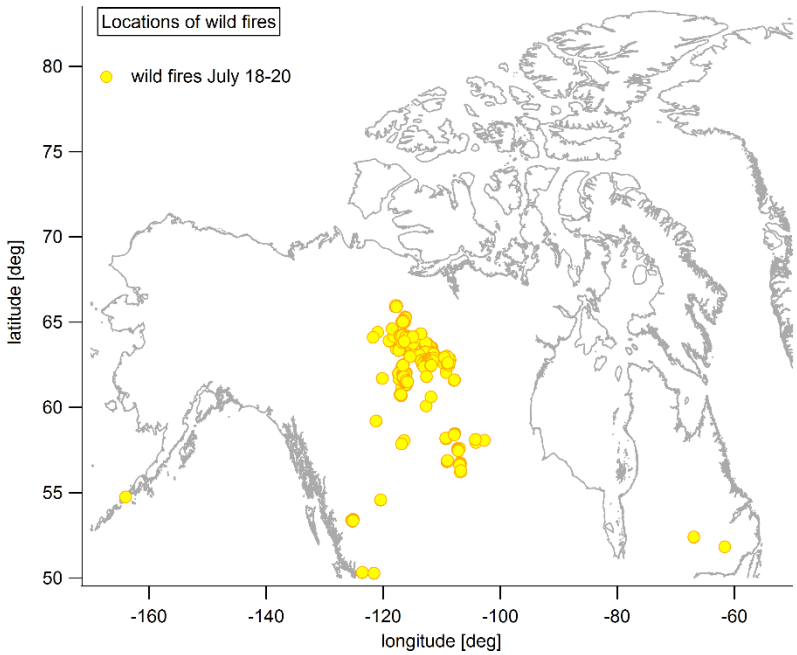

S Figure 2. Location of wild fires relevant to the southern air mass period. The data is obtained from the NASA databank (MODIS Active Fire Detections extracted from MCD14ML distributed by NASA FIRMS, available online: https://earthdata.nasa.gov/active-fire-data).

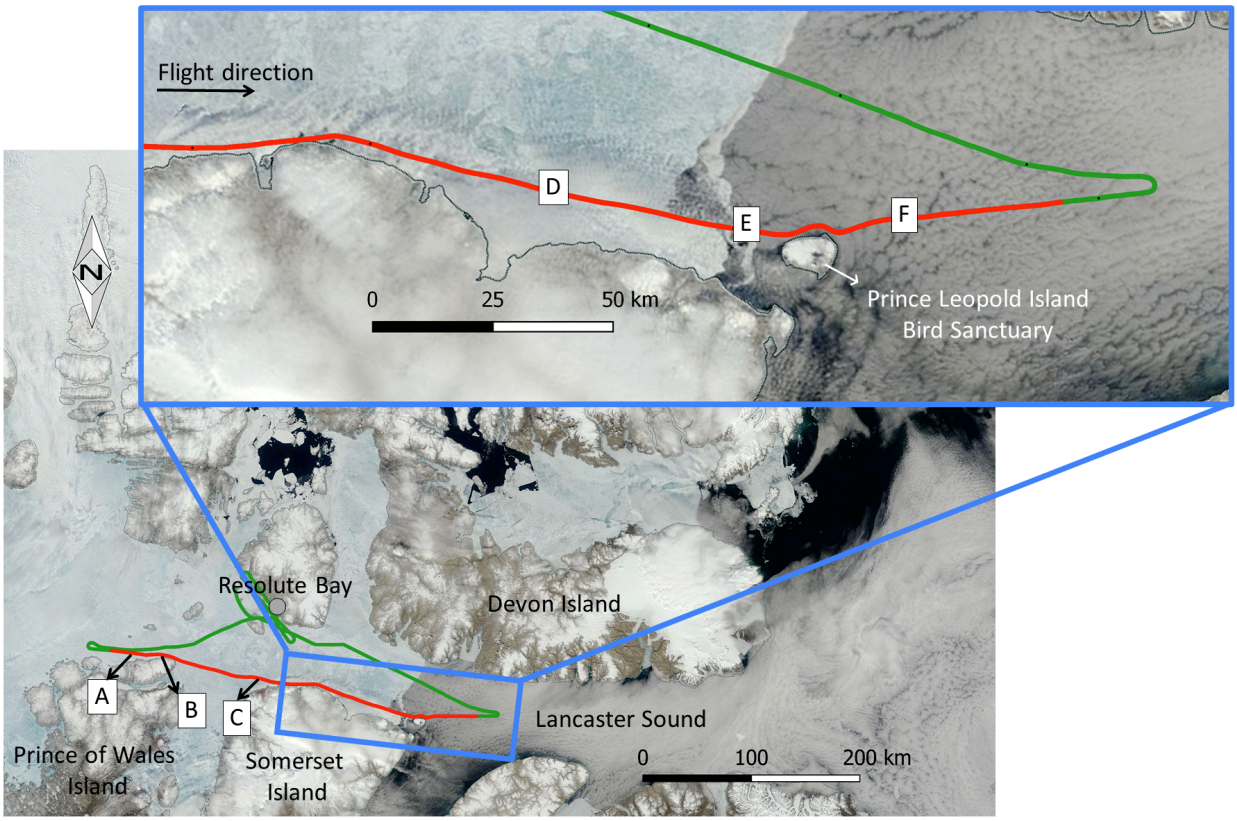

S Figure 3. Flight track of the case study on July 8. The flight track highlighted in red corresponds to the part of the flight discussed in the case study. The five locations (B)-(F) are located within the BL and air mass histories are discussed in detail. At location (A) the aircraft was still above the BL. The enlarged area shows the section where cloud patches started to reach the ice (also visible on the satellite picture) and the locations where highest concentrations of UFP were observed: (D) in cloud vicinity and (E) around the ice edge.

1131
1132

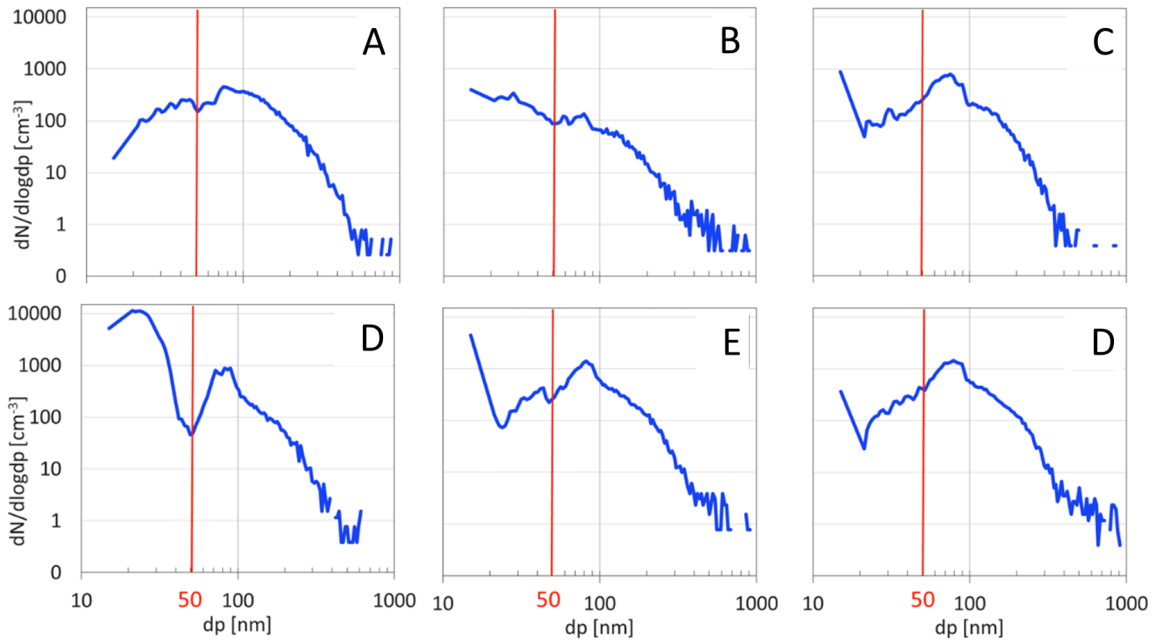

S Figure 4. Size distributions at locations A-F. Above the BL a mode of UFP is missing (A). The most pronounced mode of UFP was observed above cloud (D). At this time increased particle concentrations extend almost up to 50nm suggesting particle nucleation with subsequent growth.

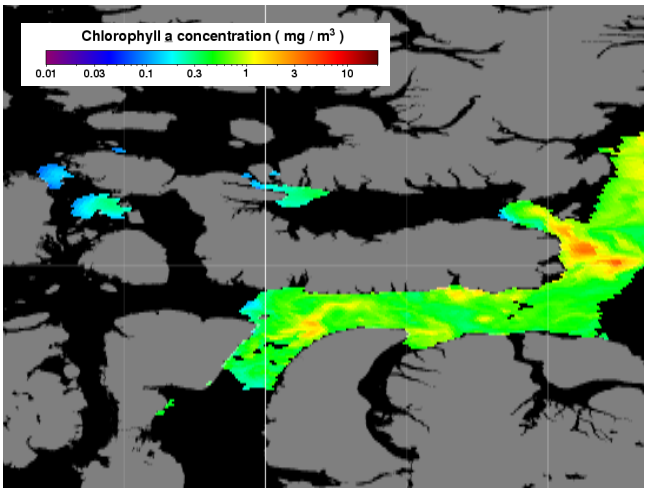

S Figure 5: Chlorophyll a concentrations on July 5th 2014 estimated from satellite measurements (Visible and Infrared Imager/Radiometer Suite) by NASA (http://oceancolor.gsfc.nasa.gov/cgi/l3).